NASA Technical Memorandum 100032

Propulsion-Induced Effects Caused by Out-of-Ground Effects

Richard Margason

December 1987

National Aeronautics and Space Administration

NASA Technical Memorandum 100032

Propulsion-Induced Effects Caused by Out-of-Ground Effects

Richard Margason, Ames Research Center, Moffett Field, California

December 1987

NASA
National Aeronautics and
Space Administration

Ames Research Center
Moffett Field, California 94035

ABSTRACT

Propulsion induced effects encountered by moderate- to high-disk loading STOVL or VSTOL aircraft out-of-ground effect during hover and transition between hover and wing-borne flight are discussed. Descriptions of the fluid flow phenomena are presented along with an indication of the trends obtained from experimental investigations. In particular, three problem areas are reviewed: 1) the performance losses sustained by a VSTOL aircraft hovering out-of-ground effect, 2) the induced aerodynamic effects encountered as a VSTOL aircraft flies on the combination of powered and aerodynamic lifts between hover and cruise out-of-ground effect, and 3) the aerodynamic characteristics caused by deflected thrust during maneuvering flight over a wide ranges of both angle of attack and Mach number.

DURING HOVER, there is a base loss caused by interactions between the lifting jets and the lower surface of the aircraft which results in a distribution of induced suction pressures which produce a lift loss. Additional performance losses include inlet flow distortion, hot-gas ingestion, hot day conditions, control bleed, internal nozzle flow, thrust vectoring, static ground effect. There are many items related to the details of the aircraft design which determine the magnitude of the losses. The aerodynamic lift loss from suction forces on the underside of the aircraft is described later.

In transition flight, there is a similar lift loss because of the interaction between the efflux of the lifting propulsive device and the aircraft's aerodynamic lifting surfaces. Extensive research has been conducted on the flow field associated with the jet in a cross-flow. The propulsion-induced effects that moderate-to-high-disk-loading STOVL and VSTOL aircraft encounter are caused by lifting jets mixing with the freestream. The research of this effect includes: 1) uniform jets, 2) nonuniform jets, 3) dual jets, 4) rectangular jets, and 5) jets in a body of revolution. Only example results will be highlighted; however, a fairly complete list of references is identified. In addition, several aspects of lateral/directional interactions are discussed. Finally these effects are considered on a complete aircraft configuration. A new aero/propulsion parameter is suggested to more completely depict the interaction effects.

BACKGROUND

The challenge of VSTOL aircraft design is an intriguing one which has been studied for many years. The first workable solution, the powered balloon, reached operational status in the 1930's and is currently receiving another look by some people. The second workable solution was the helicopter which was first demonstrated around 1940 by Igor Sikorsky and is currently the most successful application of VTOL aircraft. The third workable solution was the deflected thrust aircraft which is currently represented by the AV-8B Harrier. This paper will deal with the propulsion-induced effects encountered by the third VSTOL group of aircraft concepts which use moderate to high-disk-loading propulsion devices.

During the last 50 years NACA/NASA has conducted research specifically on the third class of aircraft. This research has focused on the development of the technology needed to identify and design feasible and practical

aircraft concepts. During this period the major advances in propulsion concepts, structures, and flight controls has enabled the consideration of an overwhelming number of configuration types. As a result, a perception has developed that nearly every VSTOL concept has been studied and been found to be impractical.

In reality many of the early VSTOL aircraft identified technology deficiencies which have since been overcome. For example, the first tilt rotor, the XV-3, had major difficulties with a rotor-induced instability. Small-scale wind tunnel models were used to develop an understanding of the coupling between the various rotor-induced instabilities and the dynamic character of the rotor/hub/pylon/wing assembly. This understanding was validated using the XV-3 as a model in the ARC 40- by 80_ft wind tunnel. By careful structural and rotor design these problems were overcome by the XV-15 and now the final development of the operational V-22 Osprey is underway. Another example, the P-1127 deflected thrust aircraft of the late 1950's had marginal performance. Through dedicated, persistent effort it evolved into the present AV-8B Harrier which is competitive with the best contemporary subsonic combat aircraft of the 1980's. To illustrate this progress, this paper will examine propulsion-induced effects encountered by high-disk-loaded STOVL configurations during flight out-of-ground effect.

The propulsion systems of STOVL aircraft must be designed to generate forward thrust for conventional flight, lifting force for hovering flight, and in many cases, additional force components for control purposes during hover, during transition between hover and wing-borne flight, and during maneuvering flight over a large angle-of-attack range. This multiple function character of VSTOL propulsion systems leads to design features which make them significantly different from conventional propulsion systems.

In most aircraft configurations, the lifting force for hovering flight is provided at two or more locations to permit moment trim and control about all three axes. This requirement is met either by location of propulsion units at several places on the aircraft (e.g., the lift/lift-cruise concept or remote augmented lift system (RALS)), or the addition of internal flow transfer ducts (e.g., the ejector or the circulation control concepts), or by use of shafts to transfer power (e.g., helicopters or tilt rotorcraft). The aircraft configurations must use the propulsion system to provide a combination of lift and horizontal thrust during transition or maneuvering flight. For conventional flight, the propulsion system provides horizontal thrust. Each of these concepts introduces its own set of problems. For example, complicated geometries for the transfer ducts which terminate in complex devices such as slots, vanes, nozzles, wide-angle diffusers, and so forth.

In all cases, the lift jets issuing from the aircraft mix with the external flow to generate extremely complicated, three-dimensional flow phenomena. In general, the jet-induced effects cause additional forces and moments on the aircraft during hover and in the transition between hover and wing-borne flight. The character and magnitude of these jet-induced effects is influenced by the flight regime being encountered as well as the specific aircraft configuration. The present paper will draw from several earlier surveys (1-5)* of VSTOL propulsion-induced effects as well as recent research results. The paper will focus on those effects which are especially pertinent to STOVL fighter or attack aircraft configurations.

This paper summarizes some of the propulsion-induced effects encountered out-of-ground effect during hover, transition, and maneuver. Descriptions of the fluid-flow phenomena are presented along with an indication of the trends obtained from experimental investigations. In particular, three problem areas are reviewed; 1) the performance losses sustained by a VSTOL aircraft hovering out-of-ground effect, 2) the induced aerodynamic effects encountered as a VSTOL aircraft flies on a combination of powered and aerodynamic lift between hover and cruise out-of-ground effect, and 3) the aerodynamic characteristics caused by deflected thrust during maneuvering flight over a wide ranges of both angle of attack and Mach number. Where there are available data, an attempt will be made to identify fundamental differences among the propulsion concepts currently being studied for STOVL combat aircraft. These propulsion concepts include; 1) vectored thrust, 2) ejectors, 3) remote augmented-lift systems (RALS), 4) tandem fan/vectored thrust, and 5) lift plus lift/cruise. Where possible some of the design conflicts among the requirements of the various propulsion concepts and the different modes of flight will be discussed, along with the present state of the art solutions to some of the problems.

*Numbers in parentheses designate references at end of paper.

AERO/PROPULSION-INDUCED EFFECTS IN TRANSITION FLIGHT

The effects caused by the interaction between propulsion efflux and aircraft aerodynamic-induced flows have been the subject of many experimental investigations. These effects are encountered in hover, during transition flight between hover and transition, and during maneuvering with vectored thrust.

During hover, there is a base loss caused by interactions between the lifting jets and the lower surface of the aircraft which results in a distribution of induced suction pressures which produce a lift loss. Additional performance losses include inlet flow distortion, hot-gas ingestion, hot day conditions, control bleed, internal nozzle flow, thrust vectoring, static ground effect. There are many items related to the details of the aircraft design which determine the magnitude of the losses. Even though the sum of these losses may only be a few percent of rated thrust, an accurate knowledge of each is required to make a realistic estimate of the aircraft performance. An error of as little as 3% in thrust would reduce the gross weight which in turn would reduce the fuel capacity and, hence, the design range by as much as 10%. This paper discusses the aerodynamic lift loss in hover which results from suction forces on the underside of the aircraft. This loss is commonly referred to as base loss.

During transition flight the lifting propulsive efflux is swept rearward by the free-stream flow and rolled into vortex pairs (Figure 1). The rolled-up vortices induce suction pressures on the fuselage and a distribution of downwash velocities over the aircraft. The downwash is in effect an induced twist angle distribution on the wing and tail as well as an induced camber over the length of the airplane.

Most of the research investigations of transition interference effects have measured the forces and moments induced by the interaction of the lifting propulsive efflux with the free stream. The general trend of these induced effects is illustrated in Figure 2. There is often a loss in lift which tends to increase with increasing forward flight velocity. There is also an increment of nose-up pitching moment which increases with increasing flight velocity. Because of the change in downwash angle in the vicinity of the tail, an additional increment of pitching moment is induced at the tail which can usually be trimmed by a tail-incidence change.

HOVER LIFT INTERACTION -The classic form of an axisymmetric free jet with a uniform nozzle-exit-velocity profile and low turbulence is sketched in Figure 3. In the jet there are two regions of flow: 1) the short potential core region (up to six nozzle diameters long) which has a conical shape and a uniform velocity profile, and 2) the fully turbulent region.

In an early program intended to evaluate base losses during hover, NASA Langley Research Center built a plenum chamber which would fit inside a rectangular fuselage (6). As a check on the effect of plenum chamber shape on jet characteristics, induced lift losses on a circular plate were obtained at an exit pressure ratio of 1.89 using the rectangular plenum chamber and using an "ideal" round plenum chamber with a large contraction ratio (36 to 1). These data are presented in Figure 4 as the "ideal" plenum--clean nozzle data and as the rectangular plenum--poor internal flow data. The "ideal" plenum chamber with a smooth, simple convergent nozzle gave a lift loss on the plate ($S/A_j = 69.5$) of a little less than 1%. The rectangular plenum chamber nozzle exiting through the same circular plate gave a large lift loss around 3%. This difference in results between the two plenum chambers caused a bit of concern.

The difference in exit pressure profiles was then identified. The "ideal" plenum chamber had a uniform dynamic pressure distribution, while the rectangular plenum chamber had a dynamic pressure profile which was depressed near the nozzle centerline. This difference was attributed to poor internal flow and internal flow separation in the rectangular plenum chamber. The internal lines of the plenum chamber were changed to improve the exit dynamic pressure profile to that presented in Figure 4. The thrust loss was reduced to approximately 1.5%. As a check to see if the character of the flow from the nozzle determined the thrust loss, the "ideal" plenum chamber had a restriction placed in its nozzle which nearly eliminated the pressure at the nozzle centerline. The lift loss increased to a little more than 1.5%. This confirmed the importance of the flow quality caused by the plenum chamber. The differences in the exit pressure profiles did not explain the lift-loss variations.

Next, an attempt was made to find a parameter which would correlate the characteristics of the core, the jet decay, and the turbulent mixing of the jet wake. The parameter chosen was the maximum dynamic pressure in the jet at different stations downstream from the jet exit nondimensionalized by the dynamic pressure at the jet exit. Data obtained at an exit pressure ratio of 1.64 from the same four plenum chamber

conditions presented earlier using the "ideal" and the rectangular plenum chambers are shown in Figure 5. The data show the dynamic pressure decay and the lift loss for circular surfaces of several sizes. At the top, the lift loss divided by thrust is plotted as a function of the square root of the ratio of surface area to the jet area. Using these parameters there is a linear variation in the data. The data for the "ideal" plenum with no restriction in the nozzle had the smallest lift loss and the slowest decay of jet dynamic pressure. The "ideal" plenum chamber with the restriction in the nozzle gave an increased lift loss and a more rapid decay of jet dynamic pressure. The rectangular plenum chamber with poor internal flow gave the largest lift loss and the most rapid dynamic pressure decay. The rectangular plenum chamber with the improved internal flow gave about the same results as the "ideal" plenum chamber with the restriction. These results indicate a relation exists between the lift loss and the rate of decay of nozzle dynamic pressure.

Both of these parameters are functions of the amount of air entrained into the jet and the proximity of the entrainment to the plate. A correlation between the slope of the lift loss curve and a parameter indicative of the dynamic pressure decay was developed. As indicated in Figure 6, this parameter is the maximum slope of dynamic pressure decay divided by the distance downstream where that slope occurs. Using the data of Figure 5, the correlation, presented in Figure 6, was obtained:

$$\frac{\Delta L_\infty}{T} = -0.009 \sqrt{\frac{S}{A}} \sqrt{-\left(\frac{\partial qx/(P_n - p)}{\partial x/d_e}\right)_{max} \left(\frac{x}{d_e}\right)_i} \qquad (1)$$

where

S = planform area

A = total jet exit area

d_e = diameter of an equivalent single nozzle having an area equal to the total of the areas of the multiple nozzles

$\left(\frac{\partial qx/(P_n - p)}{\partial x/d_e}\right)_{max}$ = maximum rate of decay of dynamic pressure

$(x/d_e)_i$ = downstream distance at which the dynamic pressure decay rate is maximum

It should be pointed out, however, that the dynamic decay parameter is quite sensitive to the details of how the data are faired. Since the magnitude of the lift loss is usually small, this error potential is not serious. The solid data symbols were obtained from a large scale test (7) which used a J-85 turbojet engine to provide a hot jet (approximately 1000°F and pressure ratios up to 1.73). The resultant lift-loss data agree with the correlation derived from small-scale data.

Subsequent investigations by Lockheed-Georgia (8) under contract to NASA on configurations derived from the XV-4B airplane show that this type of correlation can be suitable for additional configurations. However, it was determined that the effect of jet pressure ratio needed to be included in Equation 1 by multiplying the right side of the equation by $(P_n/p)^{-0.64}$ and by changing the constant from -0.009 to -0.016.

A more direct, easier to use method for estimating these hover lift losses was developed by McDonnell Aircraft (see equation in Figure 33 in Ref. 5). Correlation of data from various single and multiple jet configurations resulted in the following expression:

$$\frac{\Delta L_\infty}{T} = -0.0002528 \sqrt{\frac{S}{A}} \left[\left(\frac{P_n}{p}\right)^{-0.64} \frac{P_r t}{d_e}\right]^{1.581} \qquad (2)$$

where $P_r t$ is the total perimeter of all of jets in the configuration. It is noted that Equation 2 implicitly accounts for the higher decay rate of multiple jet configurations in terms of equivalent jet diameter but does not account for higher decay rates caused by jet exit conditions involving high entrainment rates. If higher than normal turbulence levels and decay rates are involved, Equation 1 should be used.

Most of the experimental hover data just described was obtained using simple circular jets. An investigation was conducted by Kuhlman et al. (9,10) to determine the effects of varying jet decay rate on jet-induced loads. The jet decay rate was varied using cylindrical centerbodies in the jet exit. Increased jet decay rate (Figure 7) led to an increased jet-induced lift loss on the flat plate. Jet-induced lift losses (Figure 8) reached 1% of the jet thrust for the most rapid jet decay rates for plate areas equal to 100 times the effective jet exit area. The observed lift loss versus

jet decay-rate trend agreed reasonably well with results of the previous investigations.

JET-IN-A-CROSSFLOW INTERACTION - An important aspect of estimating the aerodynamic characteristics of VSTOL aircraft in transition between hover and wingborne flight is an understanding of the flow field induced by interaction between the efflux of the lifting propulsive device and the aircraft's aerodynamic lifting surfaces. The influence of this efflux dominates the aerodynamic interaction effects for aircraft that use high disk loading devices such as ejectors, remote augmented lift system (RALS), driven fans, or turbofan/turbojet engines in hover or transition. One of the earliest attempts to analyze the jet-in-a-crossflow problem was done by Chang-Lu (11) in 1942 for a pipe discharging effluent into a stream. The analysis used discrete vortex filaments to describe the rollup of the jet wake into a vortex pair. One of the earliest experimental investigations was conducted by Jordinson (12) in 1958. A jet was injected into a wind tunnel at a deflection angle perpendicular to the free stream. Pressure was measured normal to the free stream at several planes located downstream of the jet exit.

The jet-in-a-crossflow is deflected by the free stream from the initial injection angle back toward the free-stream direction. In 1968 an experimental investigation (13) was conducted to determine the path of the jet for a range of deflection angles from 30° to 150°. As a result of this investigation an empirical equation was developed for the jet path which is a function of the effective velocity ratio and the jet deflection angle. This equation has been used with several panel methods to describe the location of the jet as a means of estimating jet induced interference effects.

In 1969 a symposium was held at NASA Langley Research Center to present and discuss data related to the flow field and analysis of a jet in a crosswind. The fifteen papers presented are available in Reference 14 and effectively summarize the early understanding of this problem. The first paper in Reference 14 has an extensive list of references of the experimental data and computational analyses available at the time. At that time most of the associated flow phenomena were identified and understood in a qualitative manner. However, a detailed quantitative description of the flow field was not available either experimentally or analytically. The rest of this portion of this paper will attempt to summarize some of the key progress achieved toward the additional understanding of this problem during the last eighteen years.

Since the 1969 NASA symposium extensive research has been conducted on the flow field associated with the jet-in-a-crossflow. For the purpose of the following discussion, this research is divided into the following areas; 1) uniform jets, 2) nonuniform jets, 3) dual jets, 4) rectangular jets, and 5) jets in a body of revolution. Only example results will be highlighted in the text; however, a fairly complete list of References (11-50) is identified.

Uniform Jets - The lift-jet/aerodynamic-surface interference problem has motivated numerous studies of a round subsonic jet of air discharging through a large plate into a uniform subsonic crossflow of the same temperature (15-36). In contrast to a jet in hover, experimental results (33) have shown that a jet exhausting into a crossflow decays more rapidly with increasing freestream velocity. A recent review (37) of the jet in a crossflow by Hancock recognizes that viscous effects dominate the real flow behavior. Inviscid analyses only provide general trends and are not useful for quantitative results or comparison with experimental results. More effort is needed on numerical modeling using Reynolds averaged Navier Stokes equations solutions. Successful computations will require careful attention to numerical diffusion because of the grid, jet-exit boundary conditions, and turbulence modeling.

One of the more comprehensive experimental studies was conducted in the NASA Langley Research Center's 14- by 22-Foot Wind Tunnel (formerly the VSTOL tunnel) by Dr. Richard Fearn of the University of Florida and many of his graduate students during the 1970's. Extensive additional research was conducted during the 1980's in cooperation with the NASA Ames Research Center. The primary goal of this program (15-22) was to provide experimental data upon which to base the development of models that would be used to predict the effects of jet/flat-plate interference.

Examples of these experimental data include measured pressures on the flat plate which are presented in Reference 17 for a 90° jet-deflection angle over a range of effective velocity ratios from 0.10 to 0.50. Measured velocities in the jet plume are presented in Reference 18 for a normal jet-deflection angle for a range of effective velocity ratios from 0.10 to 0.33. Some of the studies (21) included the effect of varying the jet-deflection angle. Measurements included velocity and pressure measurements in the plume for effective velocity ratios of 0.125 and 0.25 and for jet-deflection angles of 45, 60, 75, 90, and 105°.

Based on velocity measurements, a contrarotating pair of diffuse vortices was identified as a dominant feature of the flow field. Examples of the measured centerline and vortex curves are presented in Figure 9 for 90° (18) and 75° (21) jet-deflection angles.

A diffuse vortex model for inferring the vortex properties was developed and used to describe the vortex properties (15). A preliminary attempt to use the properties of the vortex pair to calculate the pressure distribution on the flat plate for an effective velocity ratio of 0.125 provides good agreement with experimentally determined lift and pitching-moment coefficient (16). A more complete model from Reference 22 is presented in Figure 10 showing the contours of jet-induced pressure coefficient on a flat plate at an effective velocity ratio of 0.16. The model accurately describes the measured pressure distribution using model parameters that are compatible with the known properties of the jet plume.

The jet-in-a-crossflow has applications for more than VSTOL aircraft. Some of these applications include waste discharge in streams, smoke from chimneys, fuel injection in turbine engine combustors, and reaction jets in missile control systems. Most of the investigations (12-35) can be applied to all but the last application.

For the last application, an investigation (36) was conducted over a range of effective velocity ratio from 0.03 to 1.20 using an underexpanded sonic jet with pressure ratios up to 93. The jet induced static pressure variations were measured on the flat plate for the range of effective velocity ratios at constant values of free stream Mach numbers of 0.1, 0.2, 0.4, and 0.6. A correlation of these data was accomplished by nondimensionalizing the radial distance from the jet exit to a point on the flat plate by an analytically determined distance from the sonic jet exit to the Riemann shock of the jet plume. The analytically determined plume is obtained from the following simple relation:

$$l_a/D = 0.755 \sqrt{p_{t,j}/p_\infty} \qquad (3)$$

The sample results in Figure 11 demonstrate the effectiveness of the correlation. These results indicate that the jet-interference effects of a physically similar situation can be estimated reasonably accurately for other applications.

Nonuniform Jets - It has been shown (6-10) that hover lift losses are determined by the dynamic decay characteristics of the jet. The engine exhaust dynamic pressure profiles for most STOVL propulsion concepts have nonuniform variations. Several experimental investigations (38-42) have evaluated the effects of annular, stratified, and nonuniform jets and found different induced pressures than for models with uniform initial jet dynamic pressure profiles.

The jet-in-a-crossflow investigations of Kuhlman et al. (39-40) used the jet hardware from the hover-induced-effects investigation in Reference 10 to produce an annular jet which systematically varied the jet decay rate. The decay rate was changed through the use of cylindrical centerbodies submerged in the jet nozzle at various depths below the exit plane. Jet path and induced pressures on the exit plane plate were obtained for effective velocity ratios ranging from 0.10 to 0.45. An example of the jet decay data is presented in Figure 12 and an example of the lift-loss data is presented in Figure 13(b). These results show that quicker jet decay caused little change in the induced lift loss between hover and speeds typical of wing-borne flight. Above these transition flight speeds, the jet with the quickest jet decay causes lift losses up to 45%. These results contrast with those obtained in hover (10) where increased decay rate increased the induced lift loss. The results also showed that the jet centerline trajectory turned toward the free-stream direction more rapidly as the jet decay rate increased. As a result the wake vortices are closer to the flat plate where they induce increased lift losses.

One experimental investigation (41) considered three different types of nozzle flows: 1) an annular nozzle with high-velocity core, 2) an annular nozzle with low-velocity core, and 3) a nozzle with parallel internal vanes similar to those used on the Harrier. The jet centerline paths were measured. When compared (Figure 13(b)) with the path equation from Reference 13, the first nozzle's jet penetrated nearly as far into the free stream, the second nozzle's jet penetrated slightly less, and the third nozzle's jet penetration depended upon the orientation of the vanes relative to the free stream. When the vanes were parallel to the free stream, the penetration was similar to the second nozzle. When the vanes were normal to the free stream, the penetration was less than any of the other nozzles. Small variations were measured in the magnitude of the jet-induced surface pressures adjacent to the jet exit. A concept of using an effective jet exit velocity and diameter (obtained by considering a nozzle of the same flow and thrust, but having a uniform exit velocity profile) was developed. This concept provided a means for determining the

first-order effects caused by exit velocity stratification. The results of Reference 41 suggests a method where model testing may be accomplished using uniform exit velocity profile without reproducing, in detail, the stratified exit flow characteristics of the actual propulsion system of a VSTOL aircraft.

The investigation by Schetz et al. (42) provides results similar to those of Kuhlman et al. (39-40) and disagrees with those of Ziegler and Wooler (41). Both the hover (10) and transition (39-42) experimental data show that properly modeling the correct jet decay rate is required to enable accurate simulation of aircraft efflux characteristics and proper simulation of the magnitude of jet induced loads. The Schetz results (42) indicate that the jet velocity profile is very important in determining the induced-surface-pressure distribution. The nonuniform velocity profiles increase the lift loss and decrease the induced pitching moment.

The results of these investigations (38-42) suggest that the experimental model should try to duplicate the characteristics of the actual engine exhaust under study. As demonstrated by all of these results, the appropriate characteristics are not well defined. The characteristics may include exit velocity profile, internal turbulence, dynamic pressure decay among the more important features.

Dual Jets - The effect of dual lifting jets has been investigated by Wooler et al. (33,41) and by Schetz et al. (42,43) to evaluate their effects on jet interference. Both sets of investigations included tandem jet configurations; the Schetz investigations also included a side-by-side jet configuration in the test.

An example of the in-line jet results are presented in Figure 14 and show contours of constant total pressure coefficients for a jet spacing of 7.5 diameters at an effective velocity ratio of 0.125. For these in-line jet configurations, the downstream jet decays less rapidly than the upstream jet. This difference in decay rates decreases as the jet spacing increases. The deflection in the streamwise direction and the decay of the leading jet is independent of the spacing over the range tested (33) (2.5 to 7.5 in diameter). Surface pressure data indicate that the negative pressures increase with increased spacing between the jets. As the sideslip angle is increased from 0°, the shielding of the downstream jet is reduced and there is then a greater spanwise influence of the downstream jet on the pressure distribution. Data in Reference 43 identify an additional mutual interaction between the jets. There appears to be a "swelling" of the front jet caused by the presence of the rear jet. As a result, the surface area influenced by the front jet tends to be greater than for the case of a single jet. The rear jet penetrates further into the free stream than a single jet. As a result the surface area influenced tends to be reduced from that for a single jet. The combined result is a reduced lift loss at a given effective velocity ratio from tandem jets when compared with a single jet which has the same total thrust as the pair of jets. Jet-deflection angle variation from 105 to 75° moves the effective center of the interaction region downstream.

Side-by-side jet configurations were also investigated by Schetz et al. (42,43). The gross interaction features are characterized by two interrelated effects; 1) significantly enhanced flow velocity (reduced surface pressures) between the jets because of the "channeling" of the flow between the jets, and 2) increased (when compared with the single jet) blocking of the crossflow and spillover to the sides which results in increased flow velocities (lower pressures) on the free sides of the jets. The combined result is an increased lift loss when compared with a single jet which has the same total thrust as the pair of jets.

Rectangular Jets - A few experimental investigations (45-48) of the effect of jet shape have been conducted. An early investigation by McMahon and Mosher (45) measured the effects of rectangular jet exits and compared the results with those from a circular jet. The flat-plate pressure coefficients caused by jet effects are reproduced in Figure 15(a), for a streamwise jet (aspect ratio 0.39) and circular jet, and in Figure 15(b), for a blunt jet (aspect ratio 4.42) and circular jet. For the first case (Figure 15(a)) the streamwise jet induces a less extensive negative pressure area which is centered further upstream than that for a circular jet. For the second case (Figure 15(b)) the blunt jet induces a more extensive negative pressure area which is centered further downstream than that for a circular jet.

A series of investigations (46,47) in the NASA Langley 14- by 22-Foot Wing Tunnel (formerly VSTOL Tunnel) was conducted to determine both the detailed structure and the induced effects of aspect ratio 4 rectangular jets. Test variables included nozzle orientation (streamwise or blunt), jet-deflection angle, effective velocity ratio, and nozzle test installation (flat plate or faired body). For the flat plate case, the induced pressure distributions produced results which are consistent

with results from Reference 45. Comparisons in Figure 16 of a round jet, streamwise jet, and blunt jet show that the rectangular jet distributions tend, in a qualitative sense, to "bracket" the circular jet results. The circular jet had a low-pressure wake region similar to that exhibited by the blunt rectangular jet, while the lateral spread of low-pressure and small, upstream, positive-pressure regions are more characteristic of streamwise-oriented rectangular jets. After integrating the induced effects of blunt and streamwise jets, the induced lift losses differ dramatically. The blunt jet effects are more pronounced in both magnitude and extent. These results are consistent with those for dual jets where the tandem and side-by-side arrangements correspond, respectively, to the streamwise and blunt-jet orientations.

Faired body tests were also conducted to obtain data on relatively small jet-deflection angles (between 15 and 45°). A significant effort was devoted to the design of the faired body itself to provide a relatively interference-free structure. The same plenum chamber and nozzles were used for both the flat plate and the faired body configurations. Detailed jet and vortex flow-field properties were measured at three jet-deflection angles (15, 30, and 45°). Using the procedure developed by Fearn and Weston (17), the measured velocity data were analyzed using a diffuse vortex model in a half-plane. This approach avoided vorticity cancellation by diffusion across the symmetry plane.

The resultant vorticity strengths are presented in Figure 17. The comparison indicates that the data do not agree either quantitatively or qualitatively. This disturbing result implies that changes in the jet exit configuration can dramatically alter the jet/crossflow interaction and its induced effects. The body was designed to minimize surface flow separation. However, the jet interaction may induce local circulation changes. In addition, these discrepancies imply that the flat plate, on which most jet-in-a-crossflow data have been taken, may not be as suitable a boundary condition as it has been assumed to be over the years. At these deflection angles, the flat plate may interfere with the initial formation of the vortices. What ever the reason, these results demonstrate a need for more basic research.

These basic flow-field investigations (45-47) and an investigation (48) of simple VSTOL configurations showed that a slot nozzle aligned with the free stream or several circular nozzles in a streamwise row reduced induced-lift losses and nose-up pitching moments when compared with a single circular jet. The reductions are greatest at the highest effective velocity ratios. Near hover there is very little effect. This indicates that at the greater flight speeds the vortex location further from the configuration (increased jet penetration of the free-stream flow) reduces its effect. The result of these effects is a major reduction in interference at flight speeds which approach wing-borne flight. In contrast, near hover the rectangular nozzle's greater perimeter than that for a circular nozzle causes greater viscous entrainment and induces greater lower surface suction pressures. This increase is offset by the reduced jet vortex influence and results in little difference in induced effects near hover. In summary, the rectangular jet appears to be a better exit shape than a circular exit in terms of reducing jet-induced interference effects.

Jets in Cylindrical Body - Many VSTOL aircraft configurations use lifting jets in the fuselage. The behavior of a jet exhausting normal to a cylindrical body as opposed to a flat plate represents a simple example of this configuration feature. Two experimental programs were undertaken to evaluate induced jet effects for a jet in a cylindrical body by Ousterhout (49) and by Schetz et al. (50). The first investigation used one jet in a flat plate and in a cylindrical body whose longitudinal axis was aligned with the free stream. The experimental data, taken over an effective velocity ratio range from 0.3 to 0.5, include surface pressures, lift, and pitching moment. The results in Figure 18 compare the induced results using the same 0.95-cm diameter nozzle in a flat plate and in the cylindrical body.

The induced-pressure-coefficient data (Figure 18(a)) indicate the following trends; 1) the maximum pressure coefficient is found on the flat plate, 2) the rate of pressure coefficient decay for increasing lateral distance on the surface is similar on the two surfaces, and 3) the pressure coefficient profiles for the cylindrical body extend further in the streamwise direction than the corresponding profiles for the flat plate. The induced pressures were integrated over equivalent areas for both the flat plate and for the cylindrical body and are compared in Figure 18(b). The induced lift loss is greater on the cylindrical body than it is on the flat plate at the high effective-velocity ratios.

This investigation used a small diameter jet in relation to the cylinder diameter

(D_j/D_b = 0.093). In an attempt to represent a more realistic jet in relation to the body diameter, Schetz et al. (50) used a larger jet relative to the body (D_j/D_b = 0.485) in tests conducted in the NASA Ames Research Center's 7- by 10-Foot Wind Tunnel. The main results included; 1) the maximum suction pressure decays faster with arc length around the body than with spanwise distance on a flat plate, 2) the effects of a flat-top nozzles as opposed to a contoured exit are large between the two nozzles, and 3) the rear jet was strongly sheltered by the front jet, producing lower suction pressures near the rear jet.

LATERAL AERODYNAMIC INTERACTION - In the early flight experience of the P-1127 and the XV-6A Kestrel several aircraft losses during transition flight were attributed to adverse lateral-directional characteristics. Subsequent investigations showed the existence of large-jet-induced rolling-moment instabilities and the lift losses were due to induced effects of both the lifting jets and the reaction control jets. The inlet flow causes directional instability at low speeds. These jet induced interactions are schematically depicted in Figure 19 (from Reference 51) to show the effect of sideslip on jet-induced pressures. At an angle of sideslip the jet-wake system is displaced laterally with respect to the configuration. The pressure distribution that is generated on the body, and to a lesser extent on the wing, is shifted toward the downstream side of the configuration. As a result a jet-induced rolling moment is generated. In addition there is a jet induced increment of side force and yawing moment on the body. Although the jet-wake system is usally far below the body, the force data available show that a significant sidewash is induced at the vertical tail.

Relatively little attention has been given to the jet-induced interference effects caused by reaction control jets. One such investigation (52) was conducted using control jets at the wing tip and at an inboard location on a model of a jet VTOL aircraft. The inboard control jet results are presented in Figure 20. The data show a jet-induced loss in effective roll control (Figure 20(a)) which is reduced as the control jets are moved to a rearward location (Figure 20(b)). Even greater reductions are achieved when the control jet is moved toward the wing tip near the trailing edge. Sideslipping the wing forward or upstream gave unfavorable interference increments in rolling moment, whereas sideslipping the wing backwards or downstream gave favorable increments. Aileron deflection had little effect on the interference effects between the control jet and the wing.

An investigation (53) of a VSTOL aircraft configuration with high-wing, body-mounted nacelles for lift/cruise engines, forward-fuselage-mounted lift engines, and an aft tail determined its transition aerodynamic characteristics. In addition to the longitudinal characteristics, lateral-directional-induced aerodynamic characteristics were also determined. These results were then analyzed (54) to evaluate the effect of the lifting engine efflux on the lateral control requirements of an aircraft in a 30-knot crosswind during transition between hover and wing-borne flight. At the top of Figure 21 is a plot of sideslip angle as a function of flight speed showing the increase of sideslip angle as the aircraft slows from wing-borne flight toward hover. At the bottom of the figure the rolling-moment nondimensionalized by aircraft weight and wing span is plotted as a function of flight speed. In accordance with suggested AGARD (55) hover handling qualities requirements, an available hover control power (M_x/I_x) of 1.2 radians/sec^2 is assumed to size the reaction control system in the aircraft. Then the induced transition roll control loss measured in Reference 51 is applied to determine the available roll control from the tip jets. The aerodynamic roll control caused by ailerons, spoilers, or a combination of the two is assumed to be a rolling-moment coefficient of 0.10 which combines with tip jet control moment to establish the total control available. This control power is then compared with the control requirement defined from the results obtained from wind tunnel investigation (53). The comparison shows that the available control below about 60 knots is marginal for lateral trim and does not provide adequate control power for maneuver or unexpected wind gusts.

COMPLETE CONFIGURATION INTERACTION - The magnitude of aero/propulsion interference effects is dependent on the details of the aircraft configuration. An excellent illustration is provided by the results of a classic investigation (56) of the effect of jet exit location relative to a simple wing. The investigation used a model with a simple fuselage, an unswept, untapered wing with an aspect ratio of 6 and a 30% chord slotted Fowler-type flap. The model was mounted on a sting using a strain-gauge balance. Two jets, one on each side of the fuselage, were mounted independently of the wing at about the 25% semispan station. The jet exits were positioned at each of the various longitudinal and vertical locations shown by the plus marks in Figure 22. The results of the

investigation are presented as the increment of interference lift induced by the jets at the various longitudinal locations. The results show that negative lift increments were measured when the jet exits were located ahead of the wing midchord and positive lift increments were measured when the jet exits were located aft of the wing midchord. The fact that the interference effects are most favorable for locations closest to the flap indicates that the jet is probably helping the wing and flap achieve their full lift potential.

Further experimental substantiation of the importance of jet location on induced aerodynamics was provided by a joint Navy/General Electric/NASA investigation of a VSTOL fighter model designed primarily to study lift/cruise exhaust-nozzle deflector concepts. The model used a single-lift jet in the forward fuselage and two nacelle-mounted, deflected-thrust lift/cruise jets. The results of the wind tunnel tests (57) provided performance comparisons of nozzle shapes (round and rectangular), spanwise nacelle location, chordwise jet location, and various other configuration details. The most significant effects were due to variations of jet exit locations near the wing trailing edge. The rectangular jets were located at three different positions; the baseline position and positions 15% local wing chord fore and aft of the baseline position. The results are presented in Figure 23 as the ratio of lift to thrust as a function. The dashed curve presents the combination of the vertical component of thrust and the aerodynamic lift and represents the amount of lift available if there were no aero/propulsive interference. The experimental data show that the aero/propulsive interference lift loss was reduced as the exit location was moved toward the wing trailing edge.

Configurations have been designed with rear nozzles at the wing trailing edge to gain the greatest beneficial jet interference at transition velocity ratios. An example of the improvement is presented in Figure 24. Data from the AV-6A Kestrel (58) show the detrimental jet interference typical of configurations with their nozzles located under the wing. The wing-canard configuration was designed (59) to use the beneficial jet interference from nozzles located at the wing-trailing-edge flaps. These results also demonstrated an additional benefit. In earlier unpowered wind-tunnel tests (60) this wing-canard configuration showed significant improvements in maximum lift coefficient when the canard and a canard-strake were added to the basic wing planform. However, the increased maximum lift coefficient was accompanied by rather high-static longitudinal instabilities owing to vortex lift generated by the canard-strake and flow separation over the wing-trailing-edge flaps. The two-dimensional nozzles at the wing trailing edge reduced these instabilities and also improved the lift-drag polars.

Jet-induced effects have been studied mostly for conditions representing hover and low-speed transition. In the early 1970's flight tests were conducted using the XV-6A Kestrel research airplane to study thrust vectoring in forward flight (VIFF) for increased maneuverability during high-speed flight. The Kestrel normally transitions to wing borne flight at an effective velocity ratio (V_e) above 0.36. It was observed that the predicted levels of normal acceleration were not achieved when the nozzles were vectored from their cruise position for cruise flight. This result was consistent with earlier results from wind-tunnel tests of a one-sixth-scale model of the XV-6A Kestrel (58) which showed (Figure 25) increasing aero/propulsive interference lift loss with increasing forward flight speed for the original configuration. The model was also tested with the wing moved forward to locate the rear nozzles near the trailing edge. These results show that, as the flight velocity increased, the lift loss diminishes and that the interference will become beneficial beyond an effective velocity ratio of about 0.6. Since the speeds where VIFF would be used in combat are above speeds corresponding to this velocity ratio, the potential enhancement of this configuration is evident. The AV-8B has since incorporated wing planform changes that enhance flap lift induced by jet efflux.

The data from several V/STOL configurations (57,58,and 59) are presented in Figure 26 to directly compare their transition flight characteristics. These data are presented as L/T versus V_e and the results show that the wing canard may be the best configuration. However, if the data are presented as the ratio of L/S to T/A_j and plotted as a function of $(V_e)^2$ (Figure 27), a different conclusion may be reached.

$$\frac{L}{T}\frac{A_j}{S} = \frac{C_{L,\text{power off}}}{2}(V_e^2) + \frac{A_j}{S}\sin(\delta_j) \quad (4)$$

The first term above on the right-hand side of the equation is the slope and is a function of the power-off configuration C_L. The second term is the intercept and is a function of the ratio of disk loading to wing loading. There

the higher the power-off C_L, the better the configuration should perform in transition; the larger the disk or jet area, and hence lower disk loading, the better the configuration's hover performance. For a particular STOVL configuration the aircraft designer needs to trade the hover efficiency against high-speed performance. Several features of the data in Figure 27 can be noted; 1) the $(L/S)/(T/(A_j)$ parameter is nearly linear with $(V_e)^2$, 2) the slope of the parameter is indicative of the configuration aerodynamic lift coefficient and is thus a measure of how well it might perform in transition flight, 3) the value of the parameter at the $V_e = 0$ intercept is indicative of how fuel efficiently the configuration hovers, and 4) any difference between the data and the calculated $(L/S)/(T/(A_j/S))$ indicates the magnitude of the aerodynamic/propulsive interference. The data in Figure 26 show the wing-canard configuration to have the greatest L/T at the velocities for wing-borne flight, whereas in Figure 27 it is shown to have inferior hover performance because it is a higher disk loading concept. These configurations are compared at several angles of attack and nozzle deflections in Reference 61.

Several general trends can be noted. Those configurations with nozzles at or near the wing-trailing-edge flaps have high slopes and generally beneficial interference effects indicating potentially good transition characteristics. However, these configurations tend to have small nozzle areas and a resultant high-thrust loading which make them poor hovering configurations. The Harrier-type configuration with nozzles below the wing has detrimental interference effects indicating poorer transition characteristics. In addition this format puts the magnitude of the overall aero/propulsion characteristics. While many other data nondimensionalization formats could be used, these data analyses are intended to illustrate the importance of the format selection when evaluating data from a particular STOVL aircraft or when comparing several STOVL aircraft.

CONCLUSIONS

Propulsion-induced effects encountered by moderate to high-disk-loading STOVL or VSTOL aircraft out-of-ground effect during hover and transition between hover and wing-borne flight are discussed. Descriptions of the fluid flow phenomena are presented along with an indication of the trends obtained from experimental investigations. In particular, three problem areas are reviewed: 1) the performance losses sustained by a VSTOL aircraft hovering out of ground effect, 2) the induced aerodynamic effects encountered as a VSTOL aircraft flies on the combination of powered and aerodynamic lift between hover and cruise out-of-ground effect, and 3) the aerodynamic characteristics caused by deflected thrust during maneuvering flight over a wide range of both angle of attack and Mach number. Finally these effects are considered on a complete aircraft configuration. A new aero/propulsion parameter is suggested to more completely depict the interaction effects.

REFERENCES

1. Margason, R. J., "Review of Propulsion Induced Effects on Aerodynamics of Jet V/STOL Aircraft," NASA TN D-5617,1970.
2. Barche, J., "Jet Lift Problems of V/STOL Aircraft," V/STOL Aerodynamics, AGARD CP-143, 1974, pp. 16-1 to 16-18.
3. Hickey, D. H., "V/STOL Aerodynamics: A Review of the Technology," AGARD CP-143, 1974, pp. 1-1 to 1-13.
4. Ransom, E. C. P. and Smy, J. R., "Introduction and Review of Some Jet Interference Phenomena Relevant to V/STOL Aircraft," AGARD R-710, 1984, pp. 2-1 to 2-23.
5. Kotansky, D. R., "Jet Flowfields," AGARD R-710, 1984, pp. 7.1 to 7-48.
6. Gentry, G. L. and Margason, R. J., "Jet-Induced Lift Losses on VTOL Configurations Hovering In and Out Of Ground Effect," NASA TN D-3166, February 1966.
7. McLemore, H. C., "Jet-Induced Lift Loss of Jet VTOL Configurations in Hovering Condition," NASA TN D-3435, June 1966.
8. Shumpert, P. K. and Tibbetts, J. G., "Model Tests of Jet-Induced Lift Effects on a VTOL Aircraft in Hover," NASA CR-1297, March 1969.
9. Kuhlman, J. M. and Warcup, R. W., "Experimental Investigation of Jet-Induced Loads on a Flat Plate in Hover Out-of-Ground Effect", NASA CR-159004, February 1979.
10. Kuhlman, J. M., "Variation of Entrainment in Annular Jets," AIAA Journal, Vol. 24, No. 3, March 1987.
11. Chamg-Lu, Hsiu-Chen: "Aufrollung eines Zylindrischen Strahles Durch Querwind (Rollup of a Cylindrical Jet in a Cross-wind)," Doctorial Dissertation, Univ. of Gottingen, 1942.
12. Jordinson, R.: "Flow in a Jet Directed Normal to the Wind," R. & M. No. 3074, Brit. A.R.C., 1958.

13. Margason, Richard J.: "The Path of a Jet Directed at Large Angles to a Subsonic Free Stream," NASA TN D-4919, Nov. 1968.
14. "Analysis of a Jet in a Subsonic Crosswind," NASA SP-218, September, 1969.
15. Fearn, Richard and Western, Robert P.: "Vorticity Associated With a Jet in a Cross Flow," AIAA J., vol. 12, no. 12, Dec. 1974, pp.1666-1671.
16. Dietz, William E., Jr.: "A Method for Calculating the Induced Pressure Distribution Associated With a Jet in a Crossflow," M. S. Thesis, Univ. of Florida and NASA CR-14634, 1975.
17. Fearn, Richard L. and Weston, Robert P.: "Induced Pressure Distribution of a Jet in a Crossflow," NASA TN D-7916, 1975.
18. Fearn, Richard L. and Weston, Robert P.: "Induced Velocity Field of a Jet in a Crossflow," NASA TP-1087, 1978.
19. Krausche, D., Fearn, R. L., and Weston, R. P.: "Round Jet in a Cross Flow - Influence of Jet Injection Angle on Vortex Properties," AIAA J., vol. 16, no. 15, June 1978, pp. 636-637.
20. Fearn, R. L., Kalota, C., and Dietz, W. E., Jr.: "A Jet/Aerodynamic Surface Interference Model," Proceedings - V/STOL Aircraft Aerodynamics, Naval Air Development Center, May 1979, pp.41-63.
21. Fearn, R. L. and Weston, R. P.: "Velocity Field of a Round Jet in a Cross Flow for Various Jet Injection Angles and Velocity Ratios," NASA TP-1506, October 1979.
22. Fearn, R. L., "Progress Toward a Model to Describe Jet/Aerodynamic-Surface Interference Effects," AIAA J., vol. 22, no. 6, June 1984, pp. 752-753.
23. Wu, J. C., McMahon, H. M., Mosher, D. K., and Wright, M. A.: "Experimental and Analytical Investigations of Jets Exhausting Into a Deflecting Stream," J. Aircraft, vol. 7, no. 1, Jan.-Feb. 1970, pp. 44-51.
24. Soullier, A.: "Testing at S1.MA for Basic Investigation on Jet Interactions - Distribution of Pressures and Velocities in the Jet Using the Ideal Standard Nozzle (In Unheated State)," NASA TT F-14072, 1972.
25. Soullier, A.: "Testing at S1.MA for Basic Investigation on Jet Interactions - Distribution of Pressures Around the Jet Orfice," NASA TT F-14066, 1972.
26. Thompson, A. M.: "The Flow Induced by Jets Exhausting Normally From a Plane Wall Into an Airstream," Ph.D. Thesis, Univ. of London, 1971.
27. Kamotani, Yasuhiro and Greber, Issac: "Experiments on a Turbulent Jet in a Cross Flow," AIAA J., vol. 10, no. 11, Nov. 1972, pp. 1425-1429.
28. Harms, L.: "Experimental Investigation of the Flow Field of a Hot Turbulent Jet With Lateral Flow - Part II," NASA TT F-15706, 1974.
29. Stoy, R. L. and Ben Haim, Y.: "Turbulent Jets in a Confined Cross Flow," Journal of Fluids Engineering, vol. 95, Dec. 1973, pp. 551-556.
30. Shwartz, J. and Tulin, M. P.: "Chimney Plumes in Natural and Stable Surrounding," Atmospheric Environment, vol. 6, Jan. 1972, pp. 19-35.
31. Zandbergen, T. and Joosen, C. J. J.: "Experimental Investigation of Round Turbulent Jet in a Cross Flow," NLR TR 74013, National Lucht En Ruimtevaart-Laboratorium, Amsterdam, Netherlands, 1973.
32. Smy, J. R. and Ransom, E. C. P.: "The Structure of Single Jets at Large Angles to a Crossflow," British Aerospace Report No. HSA-KAD-R-GEN 2288, 1976.
33. Fricke, L. B., Wooler, P. T., and Ziegler, H.: "A Wind Investigation of Jets Exhausting into a Crossflow - vol. I - IV," AFFDL-TR-70-154, Dec. 1970.
34. Crabb, D., Durao, D. F. G., and Whitelaw, J. H.: "A Jet Normal to a Crossflow," Imperial College, London, FS/78/35, March, 1979.
35. Chassaing, P., George, J., Claria, A., and Sananes, F.: "Physical Characteristics of Subsonic Jets in a Cross Stream," Journal of Fluid Mechanics, vol. 62, p. 41, 1974.
36. Shaw, C. S. and Margason, R. J.: "An Experimental Investigation of a Highly Underexpanded Sonic Jet into a Subsonic Crossflow," NASA TN D-7314, Dec. 1973.
37. Hancock, G. J.: "A Review of the Aerodynamics of a Jet in a Cross Flow," The Aeronautical Journal, vol. 91, no. 905, May 1987, pp. 201-213.
38. Kuhlman, J. M., Ousterhout, D. S., and Warcup, R. W.: "Experimental Investigation of Effect of Jet Decay Rate on Jet-Induced Pressures on a Flat Plate," NASA CR-2979, April 1978.
39. Livingston, D. K.: "An Experimental Investigation of a Cold Jet with Solid Center Body Emitting from a Flat Plate into a Subsonic Free Stream," M.S. Thesis, Old Dominion University, May 1975.

40. Kuhlman, J. M., Ousterhout, D. S., and Warcup, R. W.: "Experimental Investigation of Effects of Jet Decay Rate on Jet-Induced Pressures on a Flat Plate," NASA CR-158990, Nov. 1978.
41. Ziegler, H. and Wooler, P. T.: "Analysis of Stratified and Closely Spaced Jets Exhausting into a Crossflow," NASA CR-132297, Nov. 1973.
42. Moore, C. L. and Schetz, J. A.: "Effects of Non-Uniform Velocity Profiles on Dual Jets in a Crossflow," AIAA paper no. 85-1674, July 1985.
43. Schetz, J. A., Jakubowski, A. K., and Aoyagi, K.: "Surface Pressures on a Flat Plate with Dual Jet Configurations," AIAA Journal of Aircraft, vol. 21, no. 7, July 1984, pp. 484-490.
44. Kavsaoglu, M., Schetz,J. A., and Jakubowski, A. K.: "Dual Rectangular Jets from a Flat Plate in a Crossflow," AIAA paper no. 86-0477, Jan. 1986.
45. McMahon, H. M. and Mosher, D. K.: "Experimental Investigation of Pressures Induced on a Flat Plate by a Jet Issuing into a Subsonic Crosswind," NASA SP-218, 1969.
46. Thames, F. C. and Weston, R. P.: "Properties of Aspect-Ratio 4.0 Rectangular Jets in a Subsonic Crossflow," AIAA Journal of Aircraft, vol. 16, no. 10, Oct. 1979, pp. 701-707.
47. Thames, Frank C.: "Development of an Analytical Model to Predict Induced Effects of Aspect Ratio 4.0 Rectangular Nozzles in a Subsonic Crosswind," NASA CR-14582, 1978.
48. Vogler, R. D.: "Ground Effects on Single- and Multiple Jet VTOL Models at Transition Speeds Over Stationary and Moving Ground Planes," NASA TN D-3213, Jan. 1966.
49. Ousterhout, D. S.: "An Experimental Investigation of a Cold Jet Emitting from a Body of Revolution into a Subsonic Free Stream," NASA CR-2089, August 1972.
50. Schetz, J. A., Jakubowski, A. K., and Aoyagi, K.: "Jet Trajectories and Surface Pressures Induced on a Body of Revolution with Various Dual Jet Configurations," AIAA Journal of Aircraft, vol. 20, no. 11, Nov. 1983, pp. 975-982.
51. Kuhn, Richard E.: "The Induced Aerodynamics of Jet and Fan Powered V/STOL Aircraft," Recent Advances in Aerodynamics, Springer-Verlag, 1986, pp. 337-378.
52. Spreeman, K. P.: "Free-stream Interference Effects on Effectiveness of Control Jets Near the Wing Tip of a VTOL Aircraft Model," NASA TN D-4084, August 1967.
53. Margason, R. J. and Gentry, G. L., Jr.: "Aerodynamic Characteristics of a Five-Jet VTOL Configuration in the Transition Speed Range," NASA TN D-4812, October 1968.
54. Margason, R. J.: "Jet-Induced Effects in Transition Flight," Conference on V/STOL and STOL Aircraft, NASA SP-116, 1966, pp. 177-189.
55. "V/STOL Handling-Qualities Criteria," AGARD Report No. 577, June 1973.
56. Carter, A. W., "Effects of Jet Exhaust Location on the Longitudinal Aerodynamic Characteristics of a Jet V/STOL Model," NASA TN D-5333, July 1969.
57. Wooten, W. H. and Hoff, G. E., "Deflected Exhaust Jet Effects on V/STOL Fighter Performance," General Electric report number R73AEG279, July 1973.
58. Margason, R. J., Vogler, R. D., and Winston, M. M., "Wind Tunnel Investigation at Low Speeds of a Model of the Kestrel (XV-6A) Vectored-Thrust V/STOL Airplane," NASA TN D-6826, July 1972.
59. Paulson, John. W., Jr. and Thomas, J. L., "Summary of Low-Speed Longitudinal Aerodynamics of Two Powered Close-Coupled Wing-Canard Fighter Configurations," NASA TP 1535, December 1979.
60. Gloss, Blair B., "Effect of Wing Planform and Canard Location and Geometry on the Longitudinal Aerodynamic Characteristics of a Close-Coupled Canard Wing Model at Subsonic Speeds," NASA TN D-7910, 1975.
61. Paulson, John W., Jr., Thomas, James L., and Winston, Matthew M.: "Transition Aerodynamics for Close-Coupled Wing Canard Configuration," AIAA Paper 79-0336, January 1979.

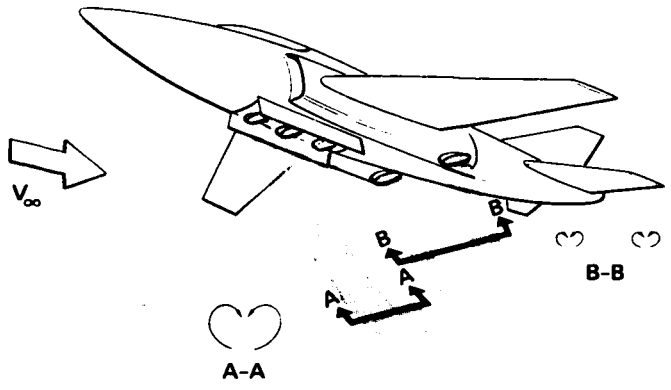

Figure 1. - Jet wakes from an aircraft in transition flight roll up into vortex pairs.

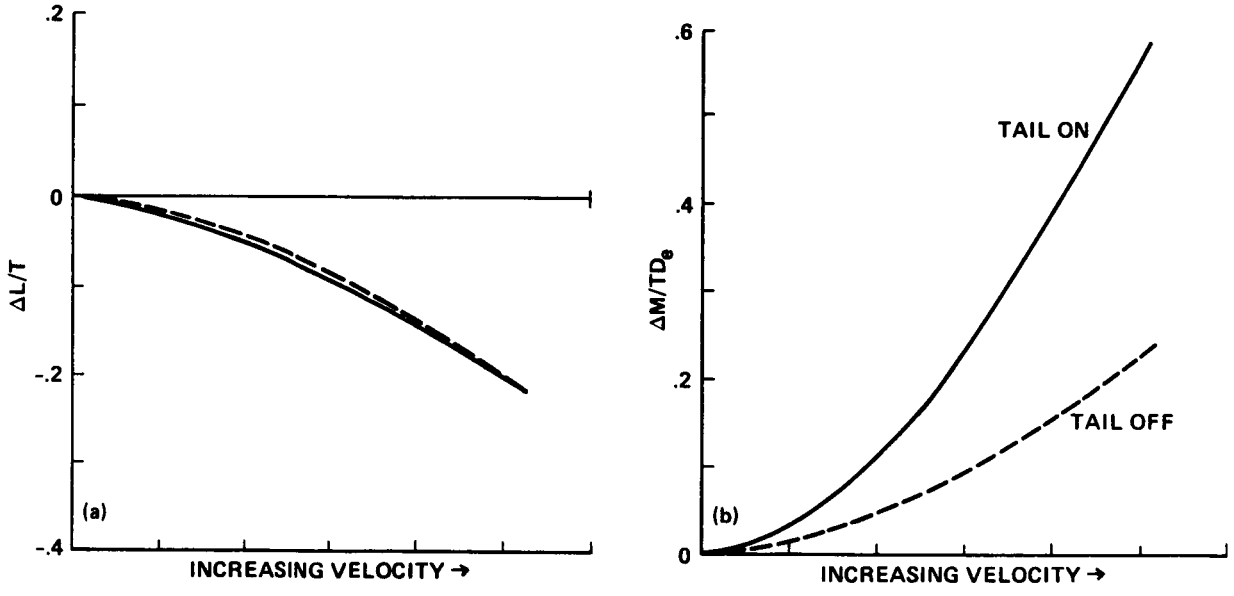

Figure 2. - The general trend of jet-induced lift loss and pitching moment in transition flight.

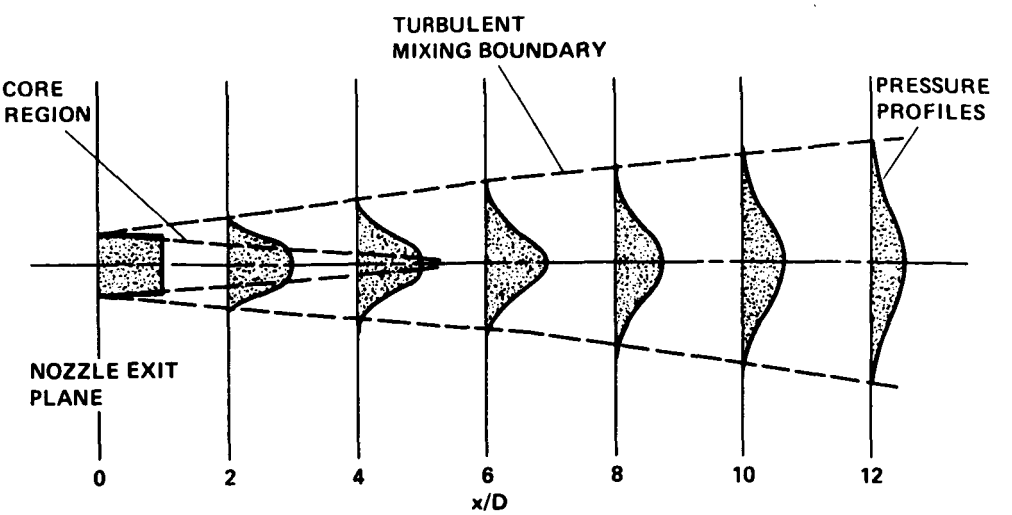

Figure 3. - Schematic sketch of the decay and spread of the jet efflux with distance downstream from the nozzle exit.

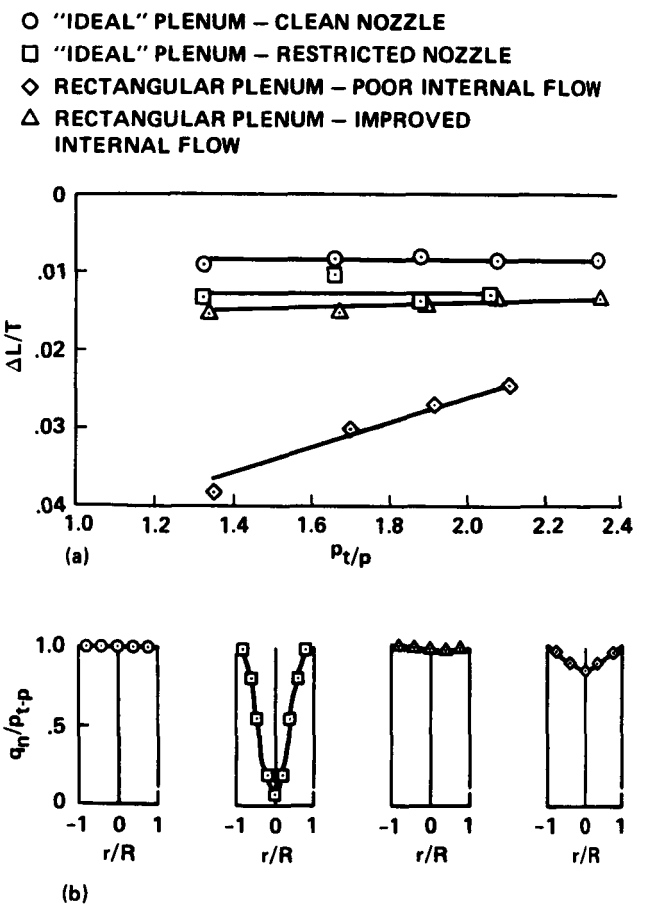

Figure 4. - Induced loads on a circular flat plate (S/A_j = 69.5) and exit dynamic-pressure distributions for several single-jet configurations ($p_{t,p}/p$ = 1.89).

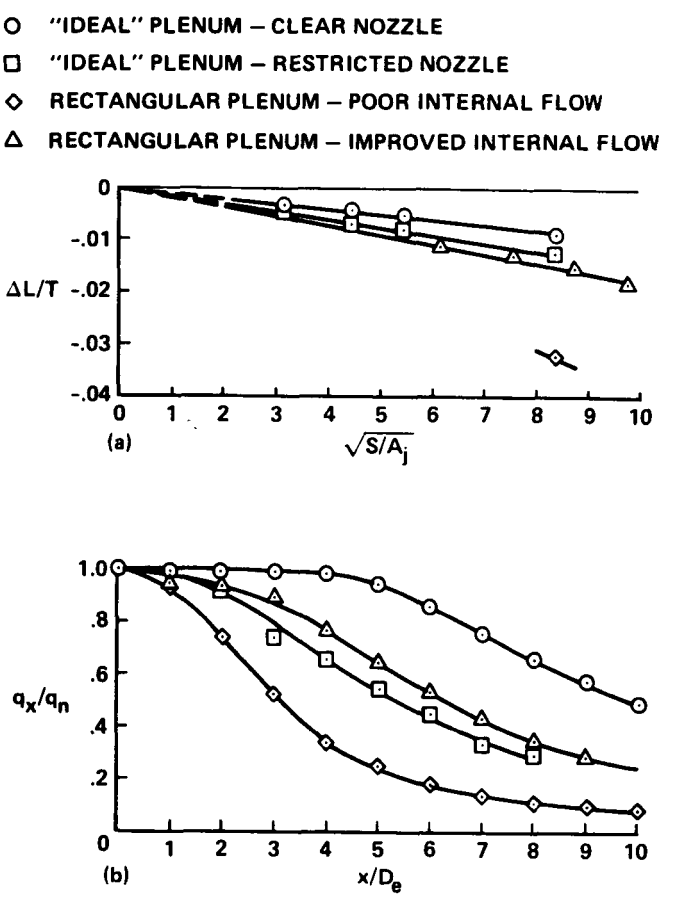

Figure 5. - Induced loads on a series of circular flat plates with several different jets exiting through their centers and dynamic-pressure decay of the efflux from these jets ($p_{t,p}/p$ = 1.64).

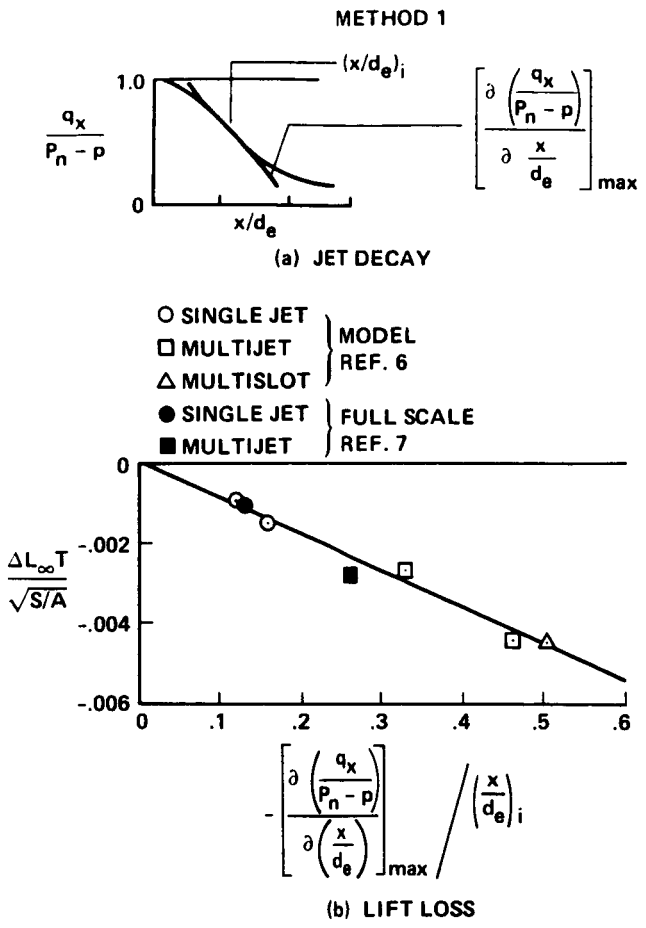

Figure 6. - Correlation of induced loads with jet decay parameter ($p_{t,p}/p = 2.0$).

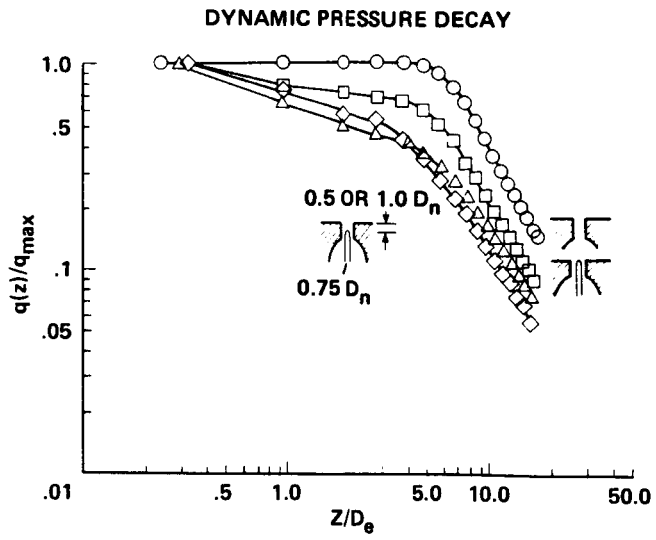

Figure 7. - Jet-centerline dynamic-pressure decay for round-tipped plug configurations in hover compared with unplugged jet.

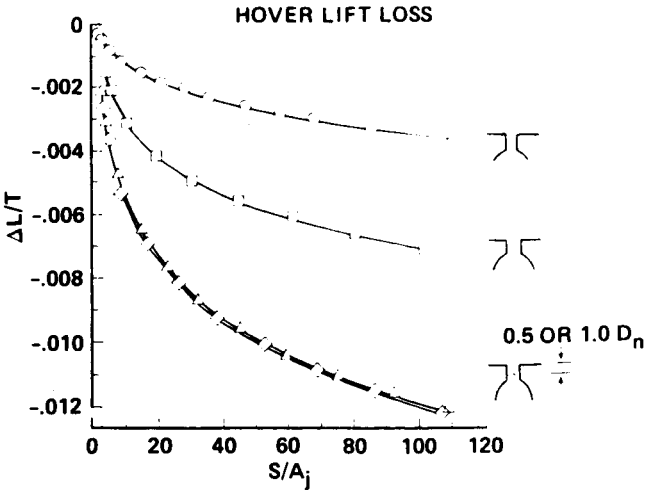

Figure 8. - Nondimensional lift loss, L/T, for round-tipped plug configurations in hover compared with unplugged jet.

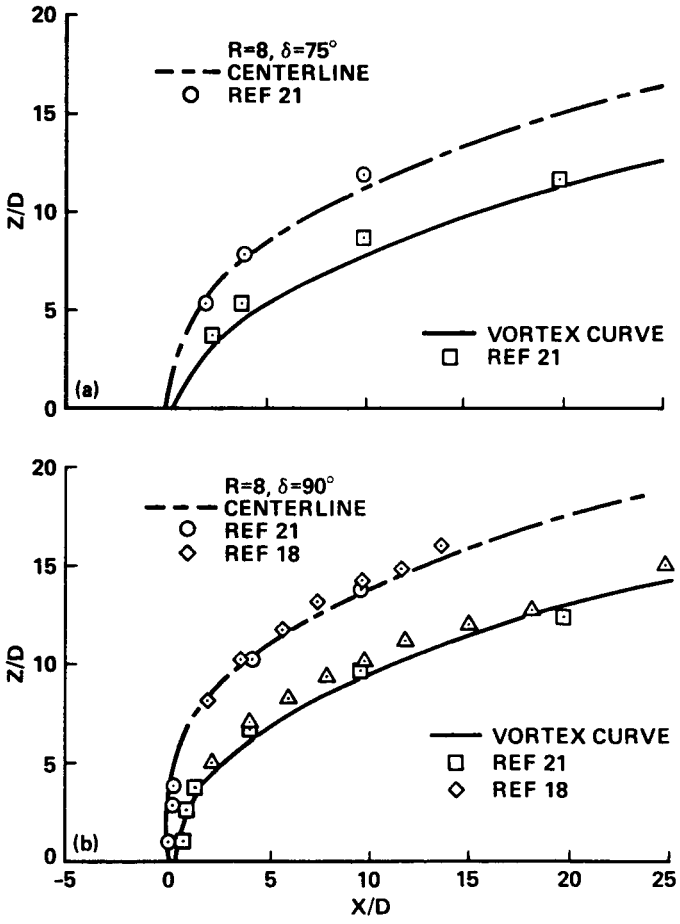

Figure 9. - Measured jet-path centerline and jet-vortex curves. (a) Jet deflection angle of 90° (18). (b) Jet deflection angle of 75° (21).

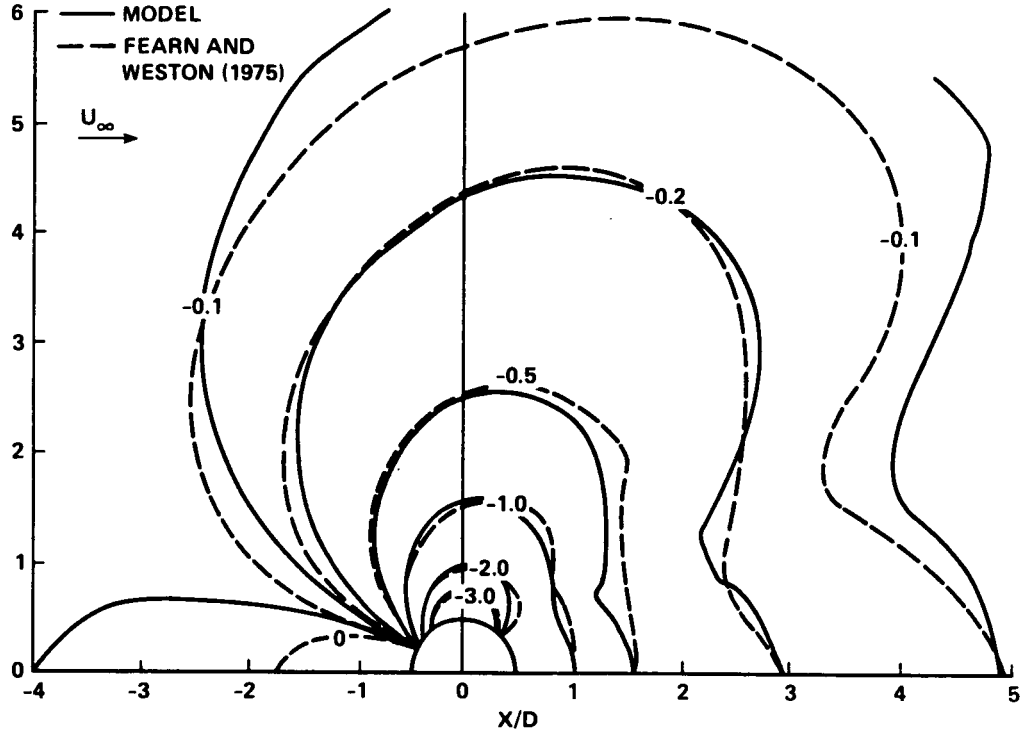

Figure 10. - Contours of constant pressure coefficient (V_e = 0.164).

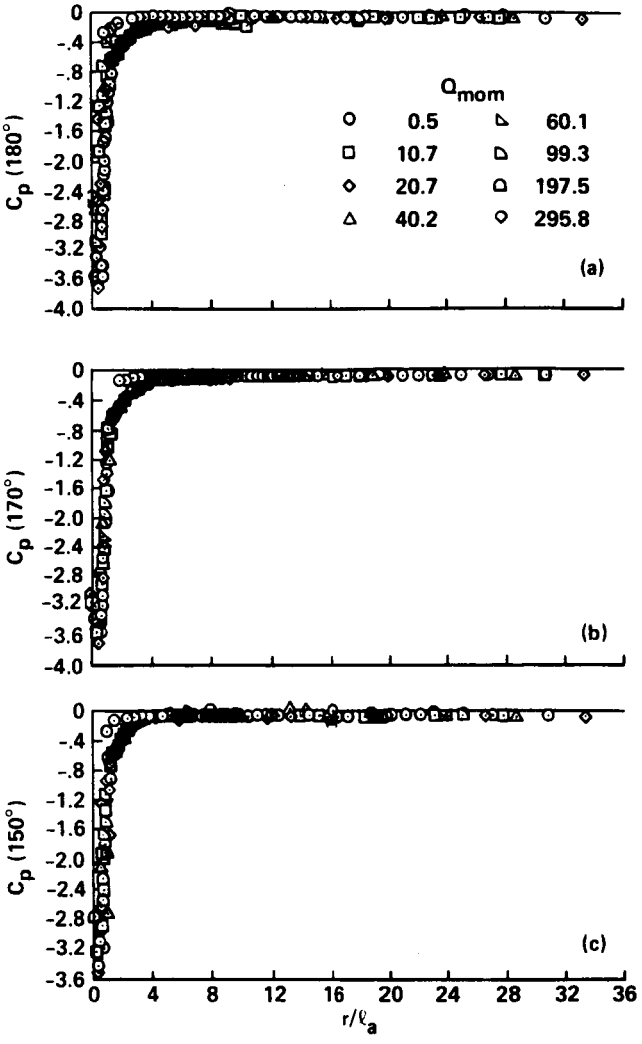

Figure 11. - Correlation of pressure coefficient induced on a flat plate by an underexpanded sonic jet over a range of effective velocity ratio from 0.03 to 1.20.

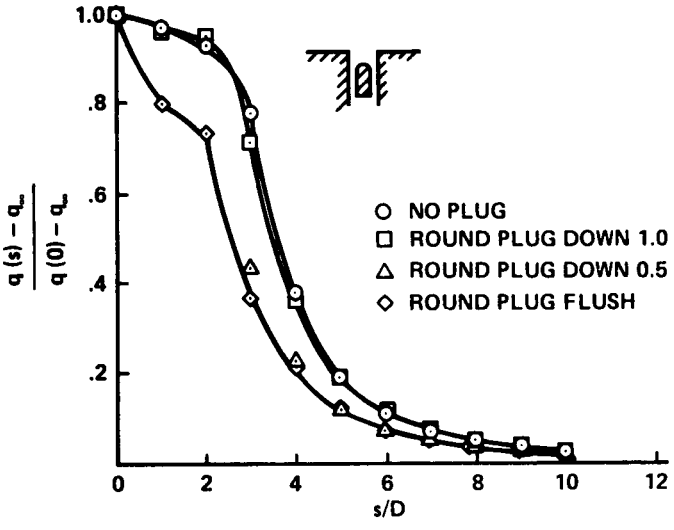

Figure 12. - Dynamic pressure decay along the jet trajectory (V_e = 0.25).

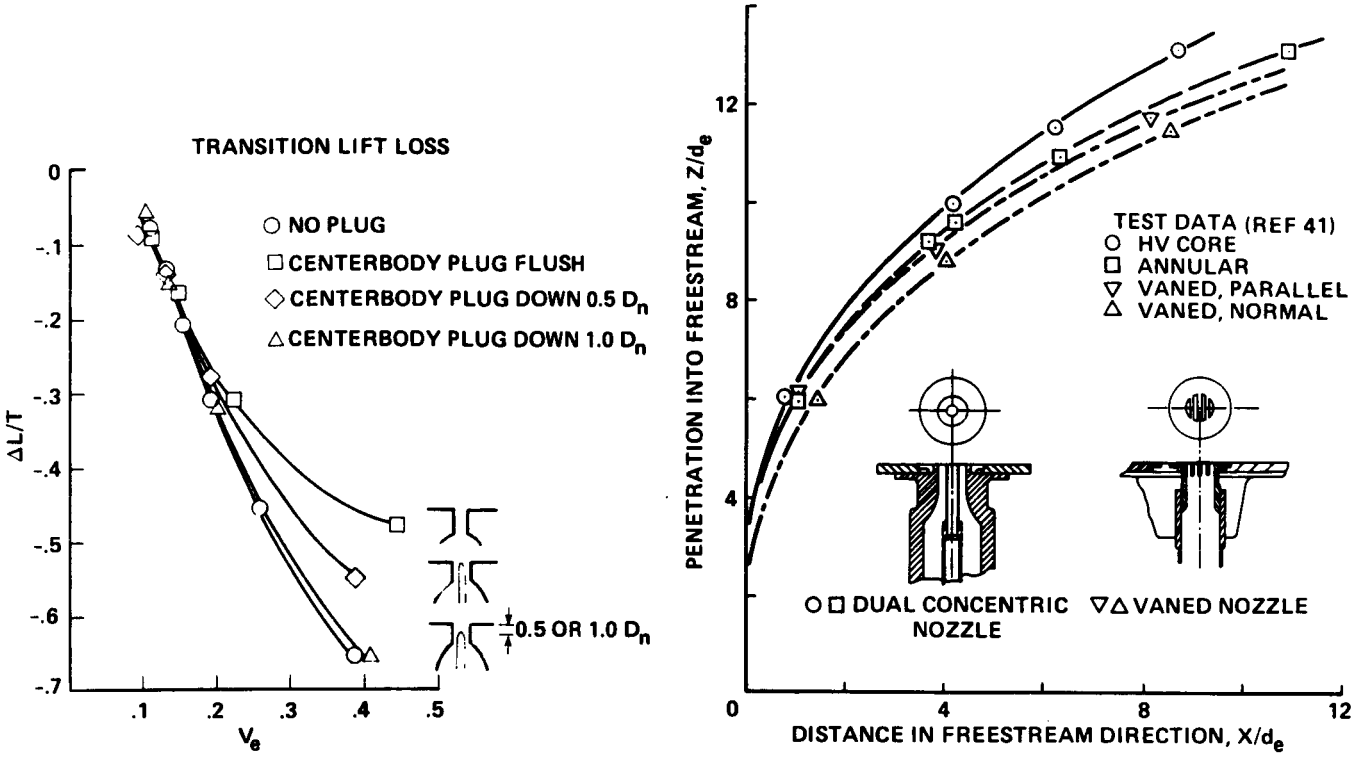

(a) Integrated lift loss for round-end plug configurations compared with a jet without a plug.

(b) Effect of jet nozzle configuration on the jet centerline paths.

Figure 13. - The effect of jet nozzle configuration on lift-jet-induced characteristics.

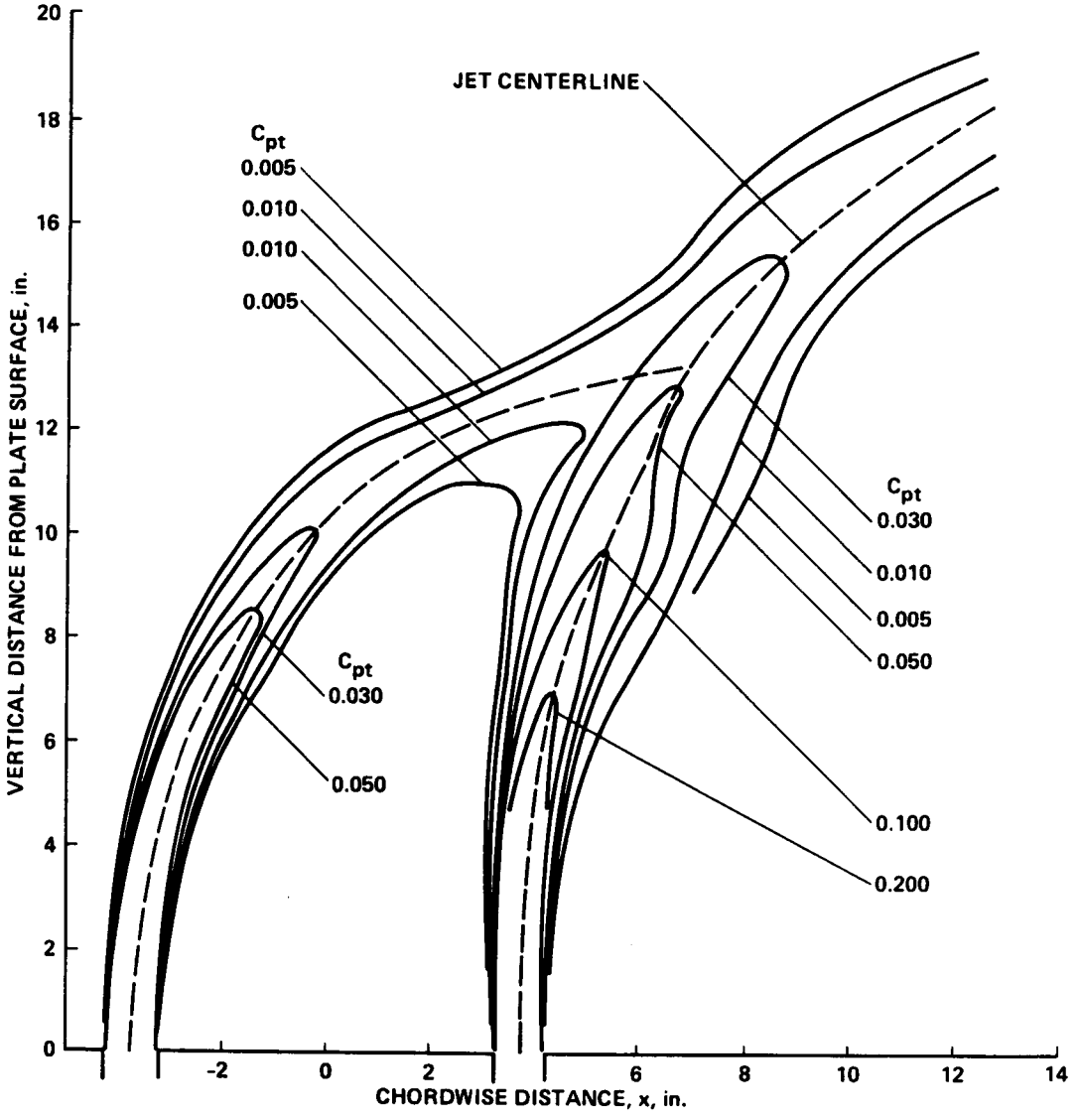

Figure 14. - Contours of constant total pressure coefficients induced by a pair of jets aligned with the free stream and with 7.5 diameters between jet centerlines (V_e = 0.125).

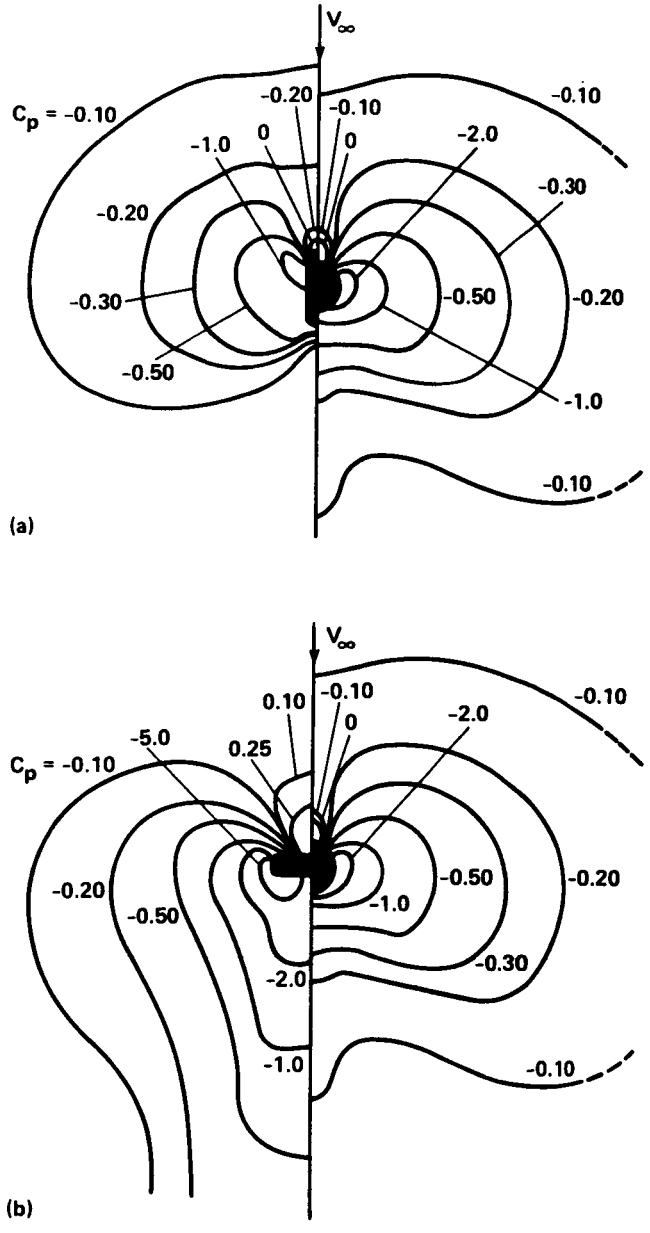

Figure 15. - Pressure distributions induced by several jet exit shapes exiting normal to the free stream (V_e = 0.125). (a) Streamwise aligned slot jet and circular jet. (b) Slot jet with its short, side-aligned streamwise (i.e., blunt) and circular jet.

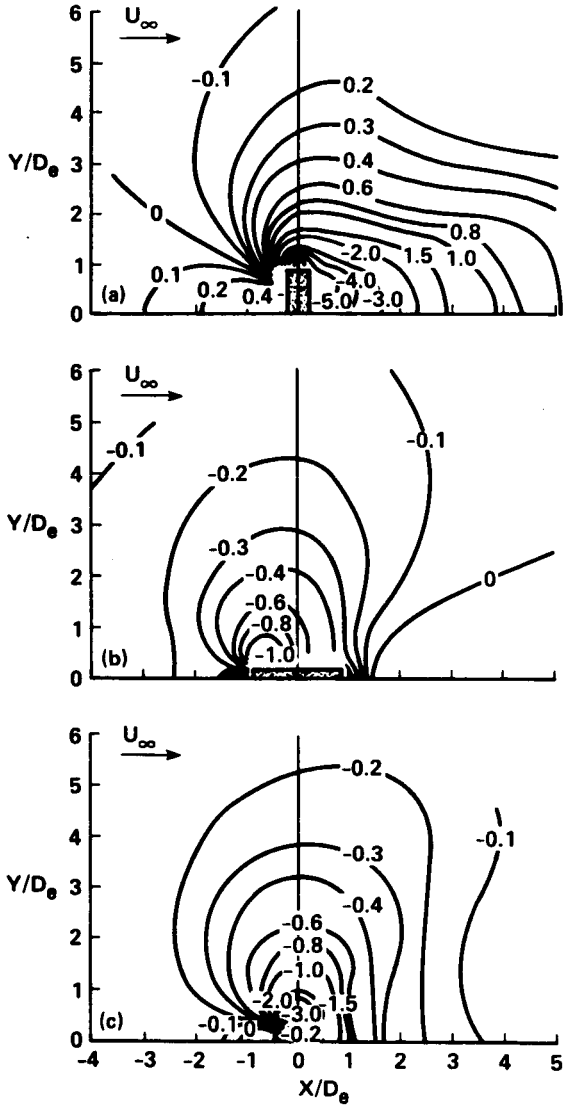

Figure 16. - Comparison of induced pressure distributions of rectangular and circular nozzles (V_e = 0.25).

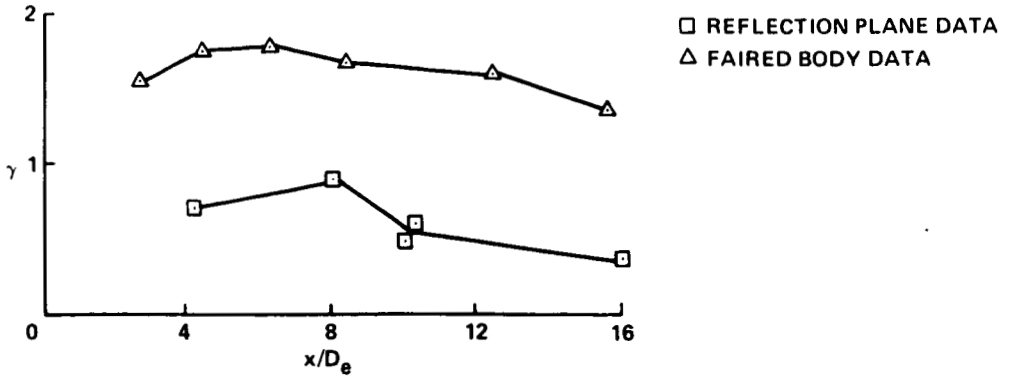

Figure 17. - Effect of the jet exit surface shape on the vortex strengths of the jets (blunt slot jet, 45° deflection, and V_e = 0.25).

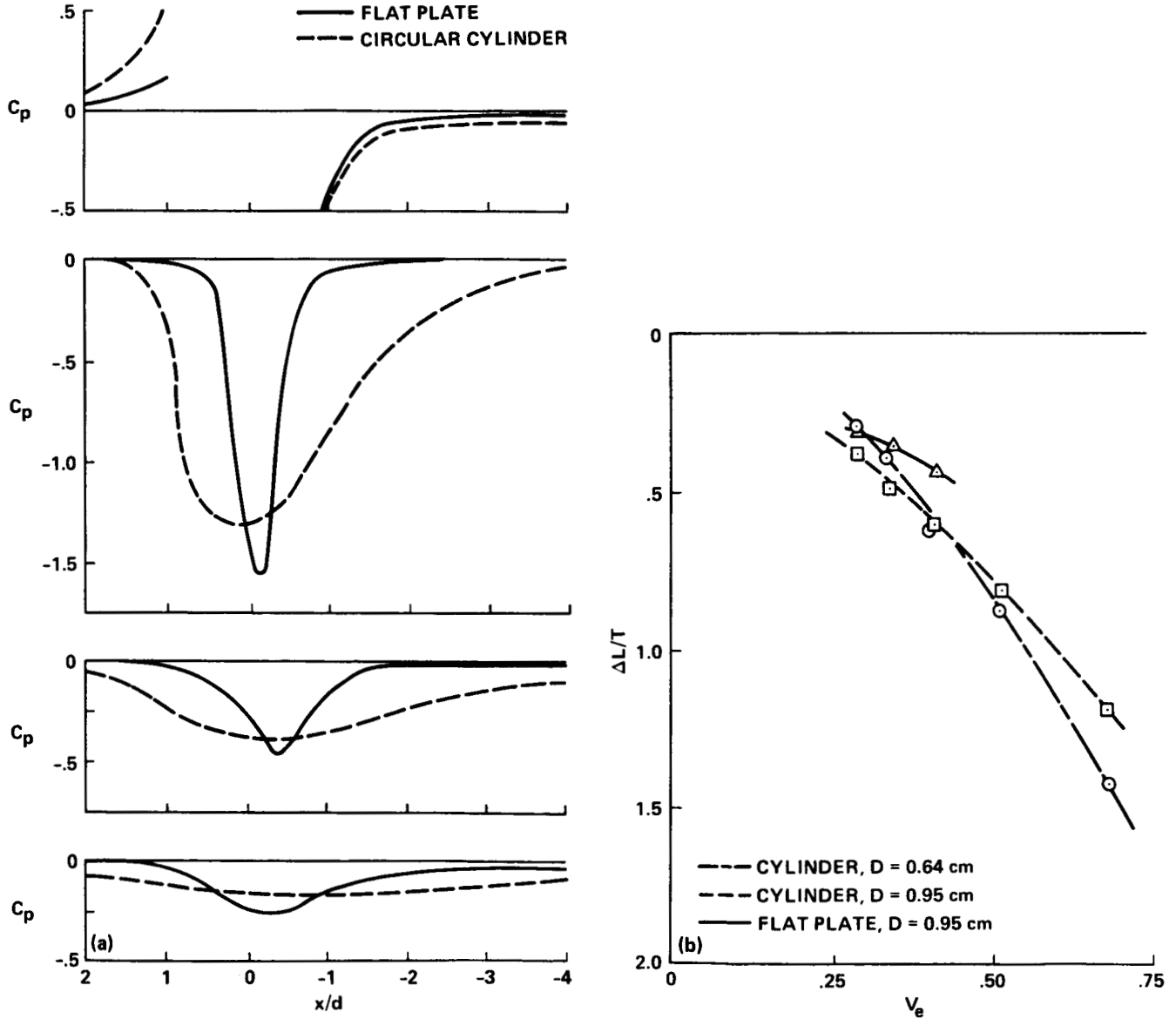

Figure 18. - Effect of the jet exit surface shape on the jet induced characteristics (V_e = 0.345). (a) Pressure coefficients induced on the surface adjacent to the jet. (b) Lift induced on the surface adjacent to the jet.

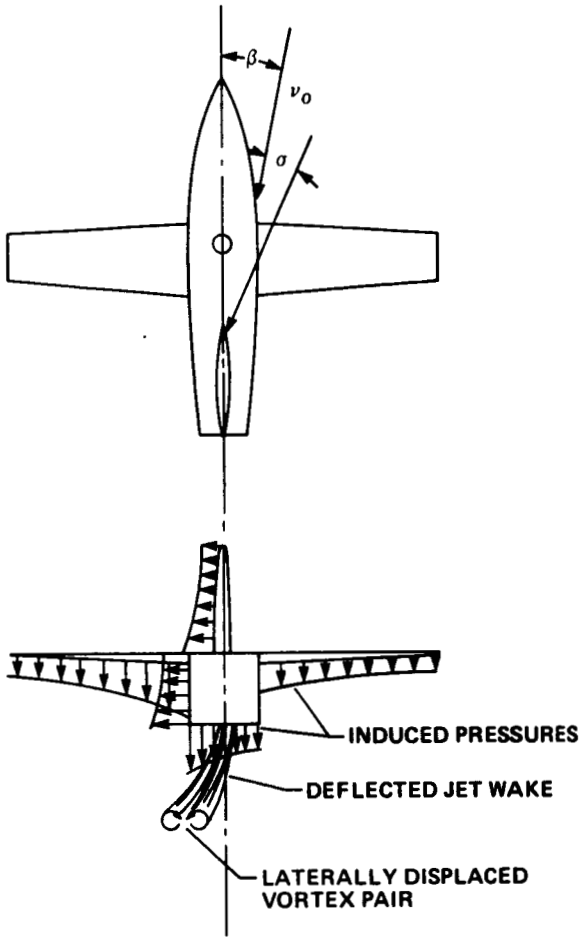

Figure 19. - Schematic of the effect of sideslip on jet induced pressures.

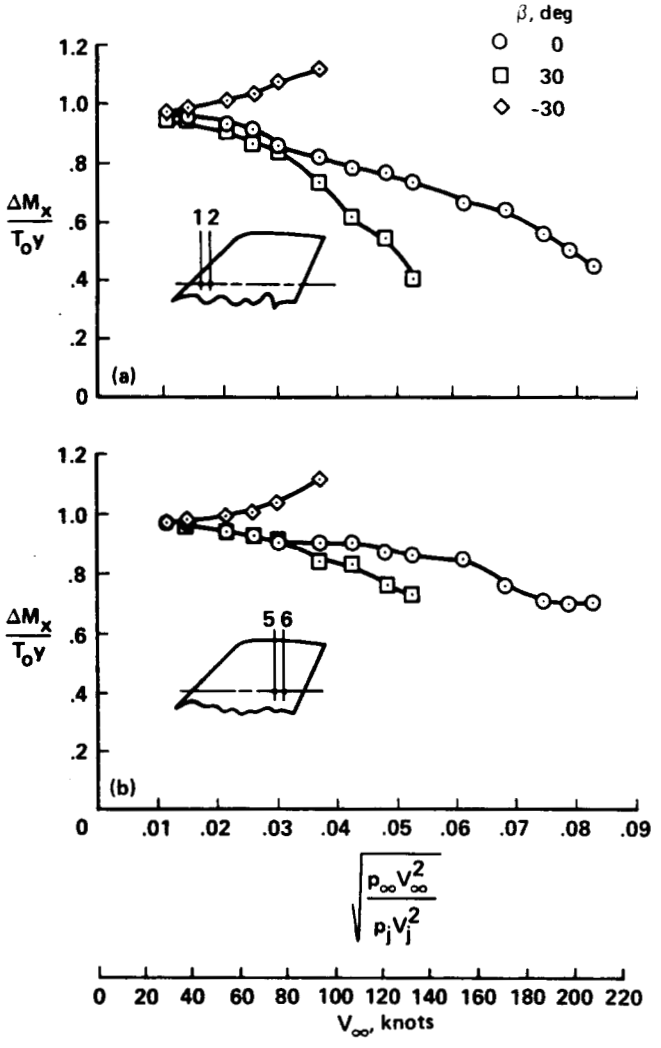

Figure 20. - Effect of sideslip on roll control through the transition speed range. Reaction control jets are located inboard of the wing tip (p_j/p = 6.0).

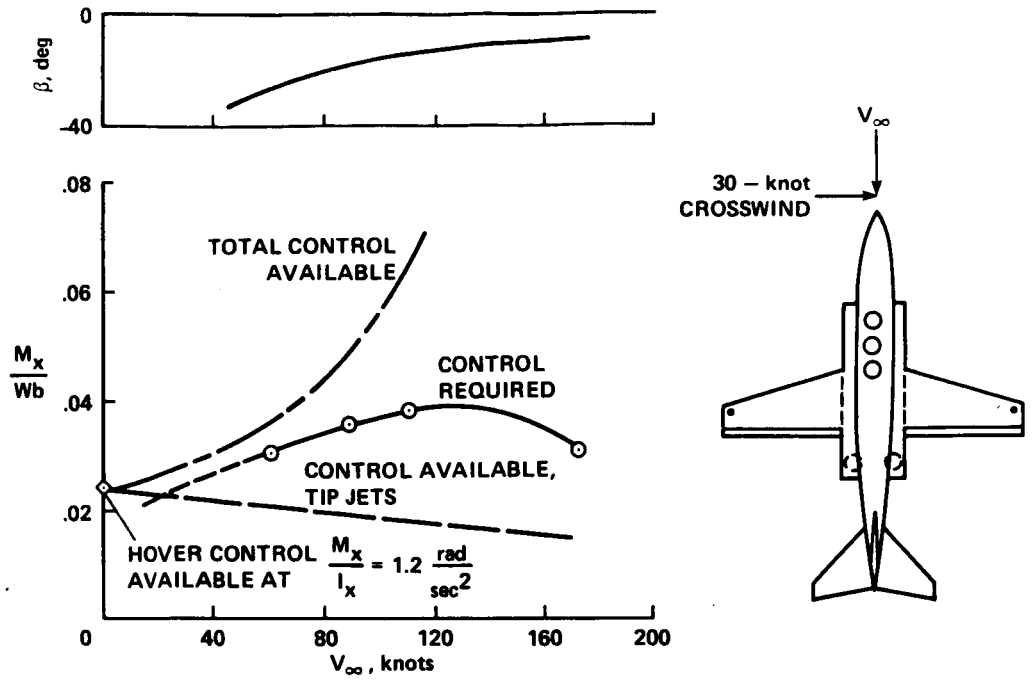

Figure 21. - Effect of power from lift-jet engines on the lateral control requirements of an airplane in a 30 knot crosswind which is transitioning from cruise flight to hover.

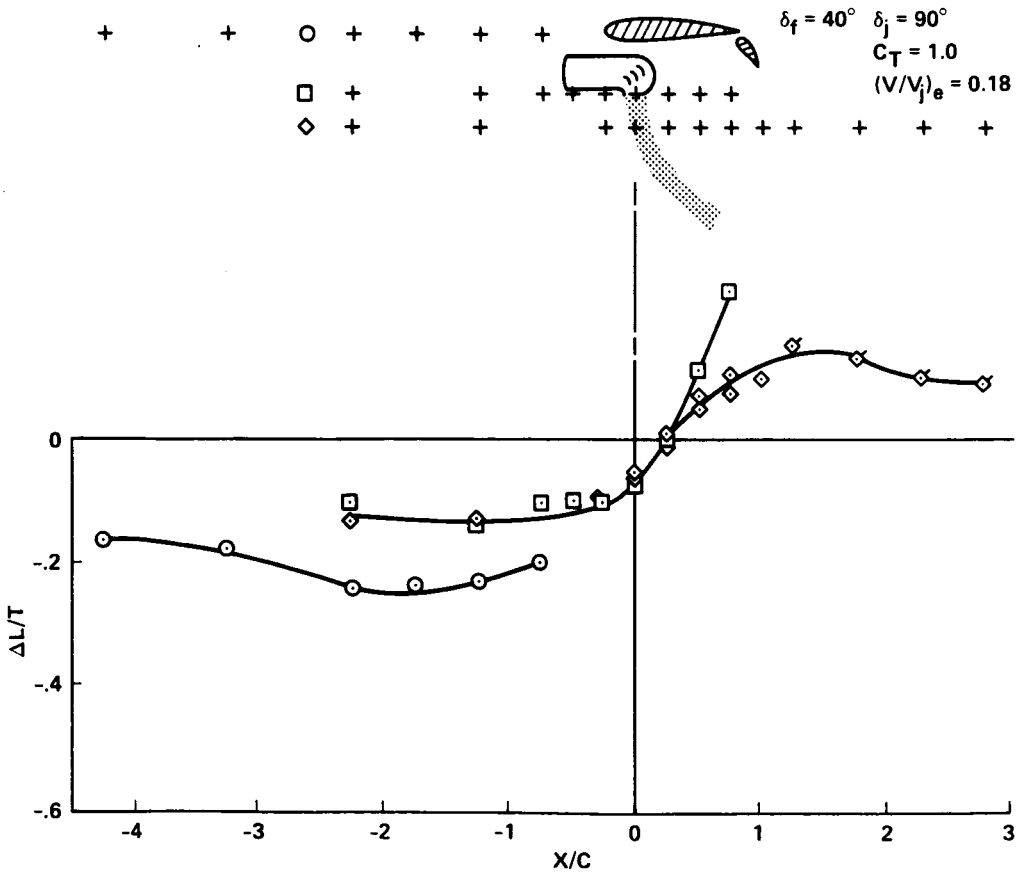

Figure 22. - Effect of varying the chordwise jet location relative to a nearby wing on the induced lift.

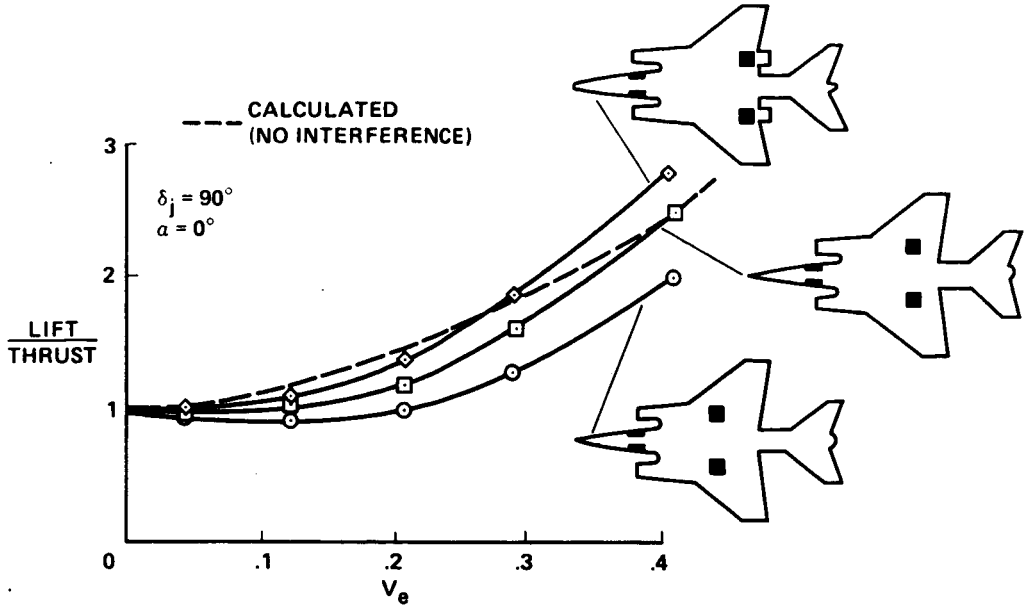

Figure 23. - Effect of deflected lift/cruise chordwise location relative to the wing trailing edge on the total lift for a supersonic combat lift plus lift/cruise VSTOL aircraft configuration.

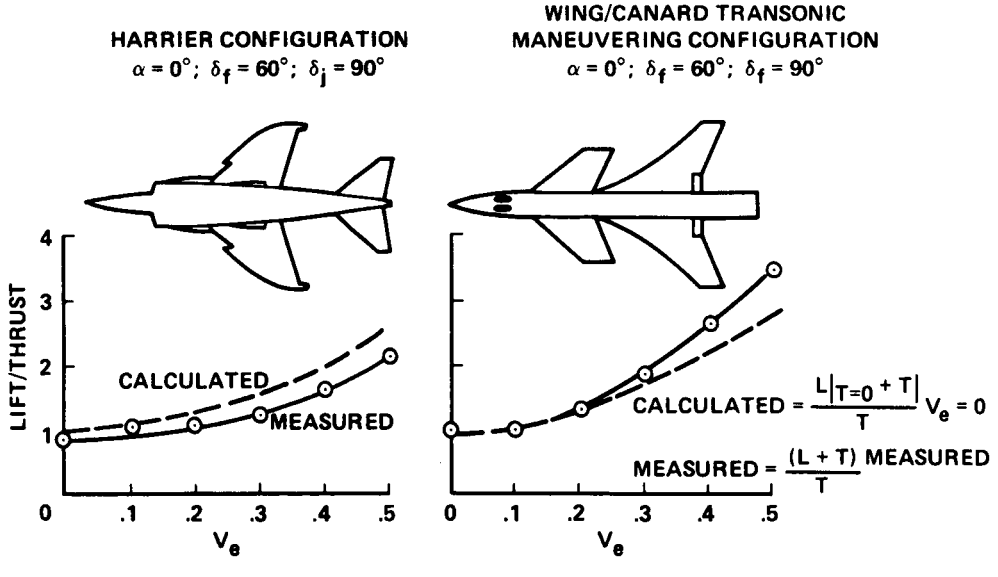

Figure 24. - Interference effects in hover and transition for both a Harrier and wing-canard combat aircraft configuration.

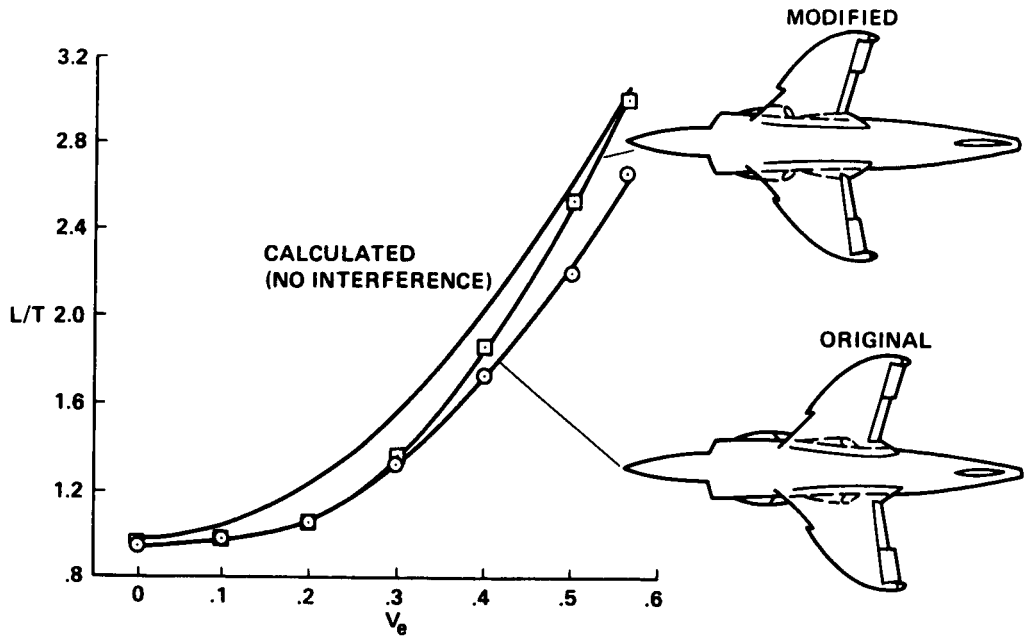

Figure 25. - Effect of a modified wing position on a P-1127 aircraft on the total lift between hover and wing borne flight.

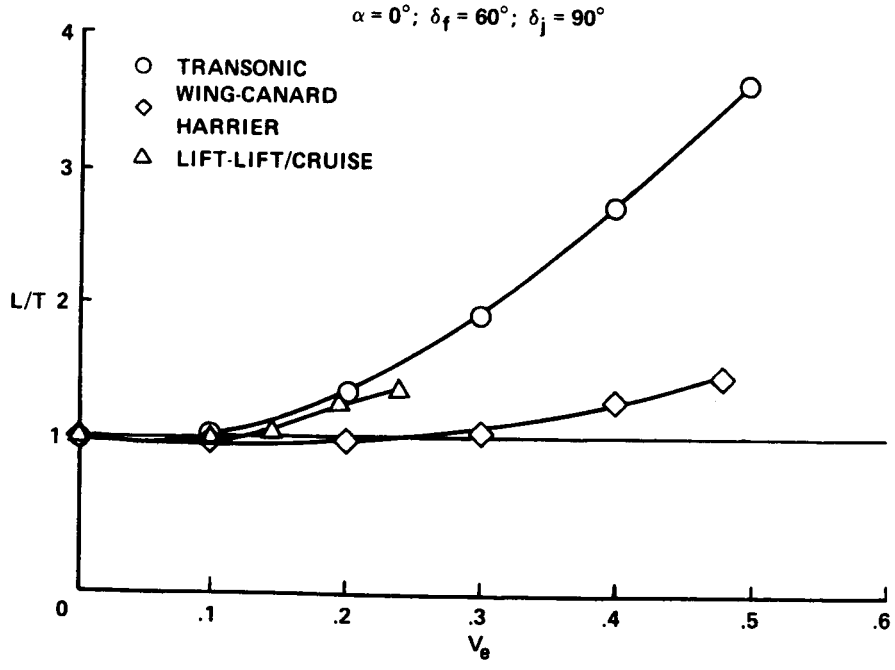

Figure 26. - Comparison of transition total L/T for three VSTOL configurations.

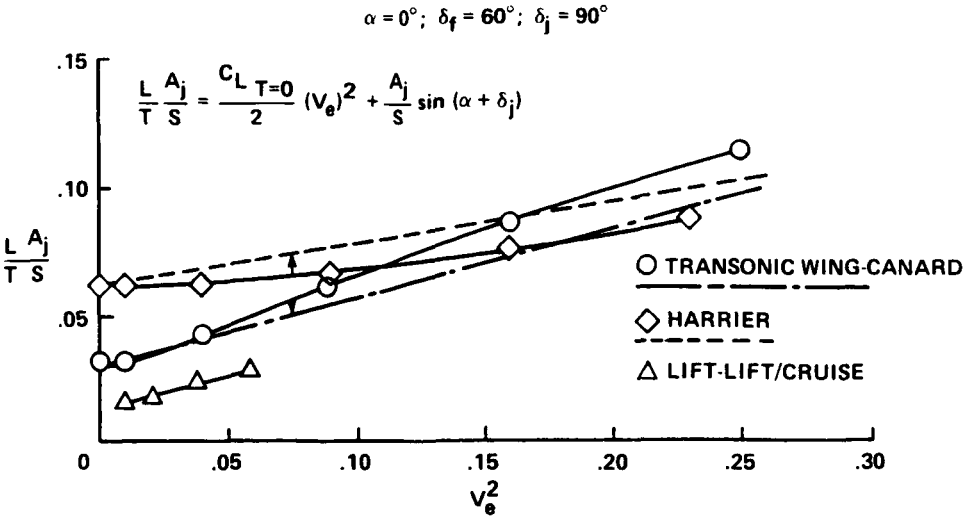

Figure 27. - Comparison of transition lift parameter $(L/T)(A_j/S)$ for three VSTOL configurations.

NASA National Aeronautics and Space Administration

Report Documentation Page

1. Report No.	2. Government Accession No.	3. Recipient's Catalog No.
NASA TM-100032		

4. Title and Subtitle

Propulsion-Induced Effects for Out-of-Ground Effects

5. Report Date

November 1987

6. Performing Organization Code

7. Author(s)

Richard Margason

8. Performing Organization Report No.

A-87359

10. Work Unit No.

505-61-71

9. Performing Organization Name and Address

Ames Research Center
Moffett Field, CA 94035-5000

11. Contract or Grant No.

13. Type of Report and Period Covered

Technical Memorandum

12. Sponsoring Agency Name and Address

National Aeronautics and Space Administration
Washington, DC 20546-0001

14. Sponsoring Agency Code

15. Supplementary Notes

Point of Contact: Richard Margason, Ames Research Center, M/S 247-2
Moffett Field, CA 94035-5000 (415) 694-5033 or
FTS 464-5033

16. Abstract

Propulsion induced effects encountered by moderate- to high-disk loading STOVL or VSTOL aircraft out-of-ground effect during hover and transition between hover and wing-borne flight are discussed. Descriptions of the fluid flow phenomena are presented along with an indication of the trends obtained from experimental investigations. In particular, three problem areas are reviewed: 1) the performance losses sustained by a VSTOL aircraft hovering out-of-ground effect, 2) the induced aerodynamic effects encountered as a VSTOL aircraft flies on the combination of powered and aerodynamic lifts between hover and cruise out-of-ground effect, and 3) the aerodynamic characteristics caused by deflected thrust during maneuvering flight over a wide range of both angle of attack and Mach number.

17. Key Words (Suggested by Author(s))	18. Distribution Statement
Powered lift STOVL Out-of-ground effect	Unclassified-Unlimited Subject Category - 03

19. Security Classif. (of this report)	20. Security Classif. (of this page)	21. No. of pages	22. Price
Unclassified	Unclassified	28	A03

NASA FORM 1626 OCT 86

For sale by the National Technical Information Service, Springfield, Virginia 22161